DksA is a central regulatory switch for stress protection and virulence in Acinetobacter baumannii

Ram Maharjan
Macquarie University
Geraldine Sulivan
Macquarie University
Felise Adams
Flinders University
Natasha Delgado
Macquarie University
Lucie Semenec
Macquarie University
Hue Dinh
Macquarie University
Liping Li
Department of Molecular Sciences, Macquarie University https://orcid.org/0000-0002-2994-6583
Francesca Short
Monash University
Julian Parkhill
University of Cambridge https://orcid.org/0000-0002-7069-5958
Ian Paulsen
Macquarie University
Lars Barquist
Helmholtz Institute for RNA-based Infection Research (HIRI), Würzburg, Germany
https://orcid.org/0000-0003-4732-2667
Bart Eijkelkamp
Flinders University https://orcid.org/0000-0003-0179-8977
Amy Cain (amy.cain@mq.edu.au)
Department of Molecular Sciences, Macquarie University

Article

Keywords:

Posted Date: April 29th, 2021

DOI: https://doi.org/10.21203/rs.3.rs-449513/v1

DksA is a central regulatory switch for stress protection and virulence in *Acinetobacter baumannii*

Ram P. Maharjan[1], Geraldine Sulivan[1], Felise G. Adams[2], Natasha Delgado[1], Lucie Semenec[1], Hue Dinh[1], Liping Li[1] Francesca L Short[3], Julian Parkhill[4], Ian T. Paulsen[1], Lars Barquist[5,6], Bart A Eijkelkamp[2], and Amy K. Cain[1]

Authors' affiliations

1. ARC Centre of Excellence in Synthetic Biology, Department of Molecular Sciences, Macquarie University, Sydney, NSW, 2109, Australia

2. College of Science and Engineering, Flinders University, Bedford Park, SA, Australia 5042,

3. Department of Microbiology, Biomedicine Discovery Institute, Monash University, Clayton, VIC, 3800, Australia

4. Department of Veterinary Medicine, University of Cambridge, Madingley Road, Cambridge, CB3 0ES, UK

5. Helmholtz Institute for RNA-based Infection Research (HIRI), Helmholtz Centre for Infection Research (HZI), 97080 Würzburg, Germany

6. Faculty of Medicine, University of Würzburg, 97080 Würzburg, Germany

[*]**Corresponding author:** Dr. Amy K. Cain amy.cain@mq.edu.au

Running Title: DksA as a major stress regulator in *A. baumannii*

Key words: stress response, global regulator, *Acinetobacter baumannii*, functional genomics, drug efflux, antimicrobial resistance

Abstract

Bacterial coordination of stress resistance mechanisms in harsh environments is key to long-term survival and evolutionary success. In many Gram-negative pathogens, both general- and specific-stress response are controlled by alternative sigma factors such as RpoS. The critically important pathogen *Acinetobacter baumannii* is notoriously recalcitrant to external stressors, yet it lacks RpoS, so the molecular control of its resilience remains unclear. Here, we used transposon insertion sequencing to characterize the molecular responses of *Acinetobacter baumannii* to two biologically-important metals stressors, zinc and copper, and discovered that the transcriptional regulator DksA acts as a major regulatory stress-protection switch. We mapped the highly pleiotropic nature of DksA using transcriptomics and phenomics and found that it controls ribosomal protein expression, metabolism of gluconeogenic substrates and survival in stresses that cause oxidative damage. *A. baumannii* strains lacking DksA were no longer virulent in both murine and *Galleria mellonella in vivo* models. *In vitro,* DksA mutants exhibited increased sensitivity to human serum and antibiotics yet promoted biofilm and capsule formation. Our study provides detailed insight into the unique role that DksA plays in stress protection and virulence for *A. baumannii* and lays the groundwork for understanding of RpoS-independent regulatory general stress response.

Introduction

Acinetobacter baumannii, a ubiquitous Gram-negative aerobe, has emerged as one of the most notorious human pathogens for health care institutions globally [1]. In the past two decades, *A. baumannii* has attracted significant attention due to its extremely high levels of antimicrobial resistance [1, 2] and has been recently recognized by the World Health Organization as one of three top pathogens in critical need of new antibiotic therapies [3]. Like many bacterial pathogens, *A. baumannii* is subject to frequently changing environments, to which it must adapt in order to survive, persist and infect [4, 5]. *A. baumannii* has a remarkable ability to survive a wide range of stresses for prolonged periods including commonly used hospital disinfectants and biocides [6], as well as those encountered during host infection e.g. metal toxicity and oxidative agents [7, 8]. Importantly, *A. baumannii* lacks well-defined host-specific virulence factors [9, 10] and its pathogenesis largely relies on its resistance to harsh environments and ability to pump out toxic chemicals via efflux mechanisms [2, 10-13]. Thus, mapping the molecular mechanisms underpinning various stress tolerance strategies in *A. baumannii* is crucial in order to ultimately tackle this pathogen.

Bacterial stress response systems are energetically costly, and large-scale defense mechanisms can involve a significant proportion of cell components to counteract environmental stresses [14, 15]. Regulation of stress adaptations at a cellular level is largely controlled by common regulators that redistribute the limited stores of RNA polymerase to transcribe genes involved in maintenance and/or survival [14, 15] via two major pathways: the general stress response, and the stringent response. In most bacteria, the general stress response system is regulated by an alternative sigma factor of RNA polymerase, RpoS (alias σ^{38} and σ^{S}). RpoS plays a pleiotropic role in the cell, activating genes involved in metabolism, protein processing, transport, and transcriptional regulation during starvation and other environmental challenges [14, 16]. The stringent response is controlled by the transcription initiating factor DksA and nucleotide alarmones guanosine penta- or tetra- phosphate (p)ppGpp [17-19],

that work together to downregulate transcription of translational machinery and reduce growth and promote expression of stress tolerance genes [17, 18, 20]. In *E. coli* and other Gram-negative bacteria, DksA and (p)ppGpp are both required for a full induction of RpoS [21-23]. While some stress responses regulated by RpoS, (p)ppGpp and DksA overlap, independent and opposing roles of DksA have also been observed, supporting the independent functioning of DksA [24, 25]. DksA has been implicated in a wide range of cellular physiology including DNA repair [26-29], amino acid biosynthesis [30], cell division [31], resistance to antibiotic [32], oxidative stress[33] and virulence in a number of Gram-negative pathogens [25, 34].

Unlike other Gram-negative bacteria, *A. baumannii* and closely related *Acinetobacter* species do not harbor a gene encoding RpoS [9, 35] and, curiously, a functional replacement for RpoS in the general stress response has not yet been identified. Here, to understand how the major stress responses are coordinated and controlled in *A. baumannii*, we chose to investigate two biologically-important metal stresses: copper and zinc. These metal ions are essential in all forms of life including in bacterial pathogenesis [7, 36, 37], yet become toxic at high concentrations [38]. Thus, host immune responses often exploit both the essentiality and toxicity of copper and zinc ions to clear invading bacteria [36, 39-44]. While excess copper is known to induce myriad of stress responses in bacteria [45, 46], zinc toxicity mainly involves oxidative stress [47].

In this study, we used transposon insertion sequencing [48] to identify genes influencing the fitness of *A. baumannii* strains under copper and zinc stresses, uncovering roles for efflux, membrane and envelope biogenesis and global regulators, including the regulator DksA. We further characterised DksA, which acts as a switch between the two stressors, using transcriptomic and phenotypic profiling of Δ*dksA* mutants and *in vivo* infection models, revealing its key role in stress protection and virulence. Our results demonstrate that DksA is not only a crucial component of the regulation

of translational machinery but also acts as an RpoS-independent general stress protection regulator in *A. baumannii*.

Results and discussion

Identification of genes important in copper and zinc stresses for *A. baumannii*

To identify the network of genes in *A. baumannii* important to survival of two infection-relevant stresses, copper and zinc, we employed the fitness-based functional genomics technique, transposon directed insertion-site sequencing (TraDIS) [48, 49]. A high-density random transposon library was generated in *A. baumannii* wild-type strain ATCC 17978 containing >110,000 unique Tn*5* mutants, and challenged with subinhibitory levels of copper (6 mM) or zinc (3 mM) for 16 h. These concentrations were chosen as the highest tolerated without significantly reducing growth rate compared to untreated ATCC 17978 (Supplementary Fig. 1). After TraDIS sequencing and analysis of frequencies of insertion mutants with the TraDIS Toolkit [50] genes whose mutants decreased in abundance relative to untreated controls were considered as necessary for metal-stress tolerance and those whose mutants increased in abundance as metal stress sensitivity (using a cut-off of 2-fold change and $P_{adj}<0.05$).

The TraDIS screen under copper stress identified 45 tolerance genes with decreased mutant fitness and 32 sensitivity genes with increased mutant fitness (Fig. 1**a**, Supplementary Table 1). Under zinc stress, 92 tolerance genes and 31 sensitivity genes were identified (Fig. 1**b**, Supplementary Table 1). To sanity-check our TraDIS genotype-phenotype screens, we identified known metal tolerance genes among the mutants with decreased abundance, such as the copper exporter *copAB* in copper treated samples (Fig. 1**c**) [51] and *czcABCD* transport genes in the zinc treated samples (Fig. 1**d**) [51, 52]. We phenotypically confirmed the validity of these control genes by comparing growth of individual, defined *copA* and *czcD* Tn*26* mutants in *A. baumannii* strain AB5075_UW [53], with and without

copper and zinc treatment. We observed altered growth only in the presence of their respective metals (Fig. 1**e**, **f**) and no growth defect compared to wild-type in untreated LB (Supplementary Fig. 2), confirming their role as metal resistance genes.

Next, we validated the growth phenotypes of a collection of single mutants that had differential abundance in TraDIS analysis previously unassociated to metal resistance, including 13 tolerance and 4 sensitivity genes for copper, and 15 tolerance and 5 sensitivity genes from zinc, using the defined mutant library in the AB5075_UW background [53]. Red colored genes with label in (Fig. 1**a**, **b)** were used for validation. A positive linear correlation with TraDIS data and screening with individual growth phenotype assays was detected in both copper and zinc conditions (Fig. 1**e**, **f**; $R^2 = 0.79$ in copper and $R^2 = 0.57$ in zinc, Supplementary Fig. 2), indicating that the TraDIS results accurately predict the phenotypic impact of zinc or copper stress on individual mutants, even across distinct *A. baumannii* strains.

Besides the known copper and zinc efflux genes, the TraDIS analysis also identified a number of genes involved in other cellular functions including cell wall/envelop/membrane biogenesis, and global regulators involved in translation and ribosome synthesis for both copper and zinc stresses (Supplementary Fig. 3). These data indicated that no single pathway can fully account for the *A. baumannii* metal tolerance profile, and multiple layers of gene regulation are required for adaptation to metal stresses. While the copper and zinc stress responses involved distinct gene networks, we also found some shared metal tolerance genes. For example, Tn*5* insertions in genes associated with membrane integrity and capsule synthesis (*wzb*, *galU, pgi* and *lptE*) were depleted in both copper and zinc stress (Fig. 2**a**, Supplementary Table 1). Similarities of metal sensitivity genes were also observed, for instance, disruption of *dcaP,* an outer membrane pore forming protein for nutrient uptake [54], increased tolerance to both copper and zinc (Fig. 1**e**, **f**; Supplementary Fig. 2).

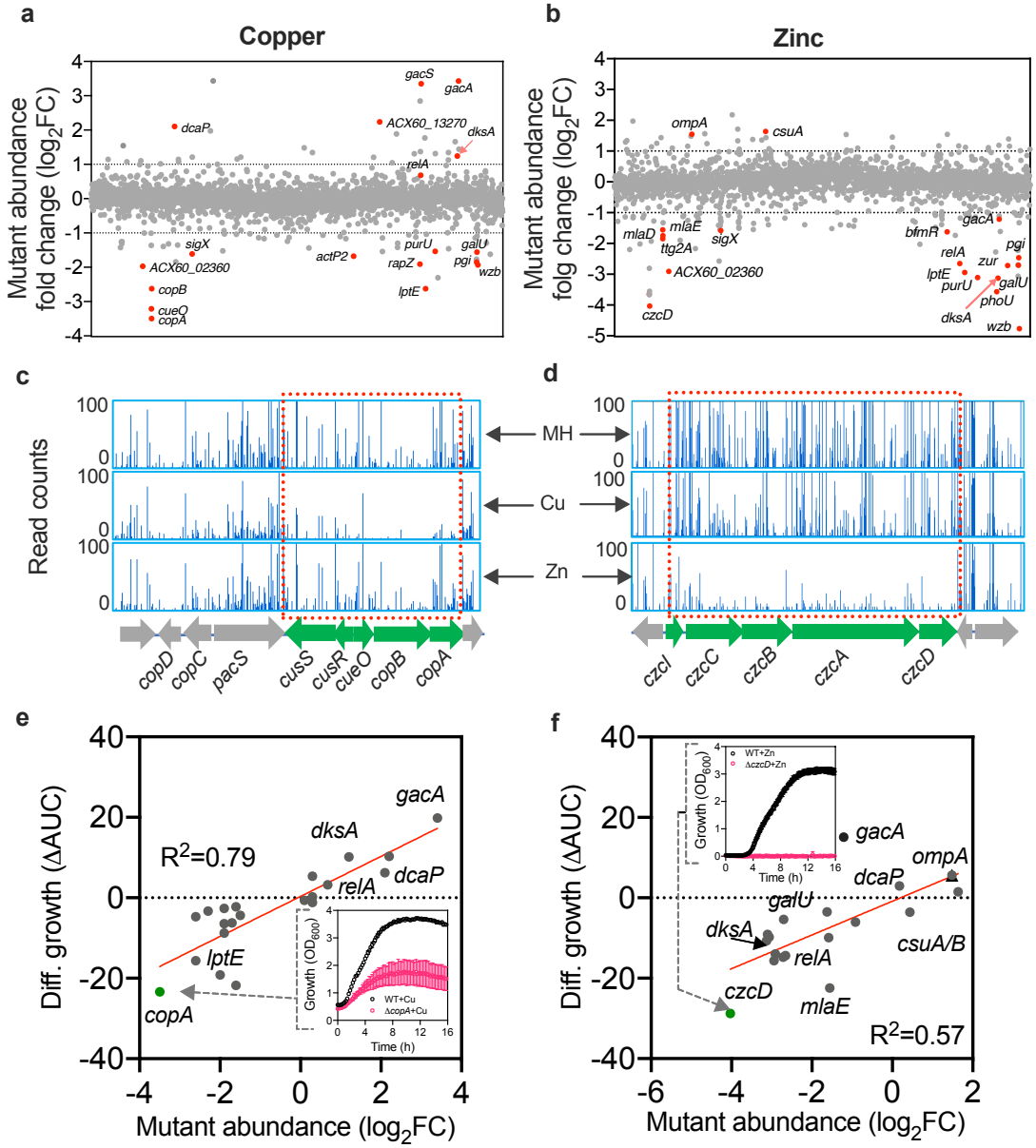

Figure 1. Identification and validation of *A. baumannii* genes that alter fitness under copper and zinc stresses using the TraDIS approach. The effect of 6 mM $CuSO_4$ (**a**) and 3 mM $ZnSO_4$ (**b**) on the abundance of transposon insertion mutations (differential abundance of Tn*5*, log_2 fold change (FC)) mapping to the *A. baumannii* ATCC 17978 chromosome and plasmid pAB3 as determined by TraDIS analysis. Examples of TraDIS plots mapping at the known copper (**c**) and zinc (**d**) detoxification loci *copAB* and *czcCBDA* of *A. baumannii,* respectively. Top panel in (**c**) and (**d**) represents read counts reflecting growth of the ATCC 17978 TraDIS library in the control Mueller Hinton (MH), whereas middle and bottom panels represent read counts under copper and zinc stresses respectively. Validation of TraDIS results using independent single gene inactivated mutants of *A. baumannii* strain AB5075_UW in copper (**e**) and zinc stress (**f**). Growth differences (measured as a

difference in area under curve, ΔAUC) between the wild-type AB5075_UW and Tn*26* insertion mutants in presence of $ZnSO_4$ or $CuSO_4$ was used as a proxy for fitness of the single gene inactivated mutants. Red colored genes with label in (**a, b**) were used for validation. Insets showing examples of growth curves of wild-type and its *copA* and *czcD* mutants in presence of 3 mM $CuSO_4$ and 1.5 mM $ZnSO_4$ respectively. Each data point (open black and peach circles and error bars) represents mean and standard deviation from at least three independent assays. Each Tn*5* mutant fitness in (**a**, **b**) value was calculated from two independent TraDIS experiments. See Supplementary Fig. 2 and methods for further details.

Only two potential global regulators were identified that showed opposite effects in copper and zinc stresses: the two-component system *gacS/A* and transcriptional regulator *dksA.* While *gacS/A* has been studied extensively in *A. baumannii* and is known to be a dynamic coordinator of tolerance to stress, virulence, motility and antibiotic resistance [11, 55], the role of DksA is largely uncharacterized in *A. baumannii*. The TraDIS data suggested that DksA may act as a molecular switch in responses to the two similar but distinct metal stress conditions (Fig. 2**b**). Phenotypic fitness assays of the *dksA* mutant confirmed that DksA disruption is deleterious to the bacteria under zinc stress (Fig. 2**d**), whereas it is beneficial under copper stress (Fig. 2**e**). We further noticed that the Δ*dksA* mutant had a comparable growth rate to wild-type but reached stationary phase much earlier than wild-type with a significantly lower growth yield (Fig. 2**c**). Since host immune cells exploit the sensitivity of bacteria to metal stress during infection, we further investigated the role of DksA as a potential molecular switch, coordinating stress protection and virulence in *A. baumannii*.

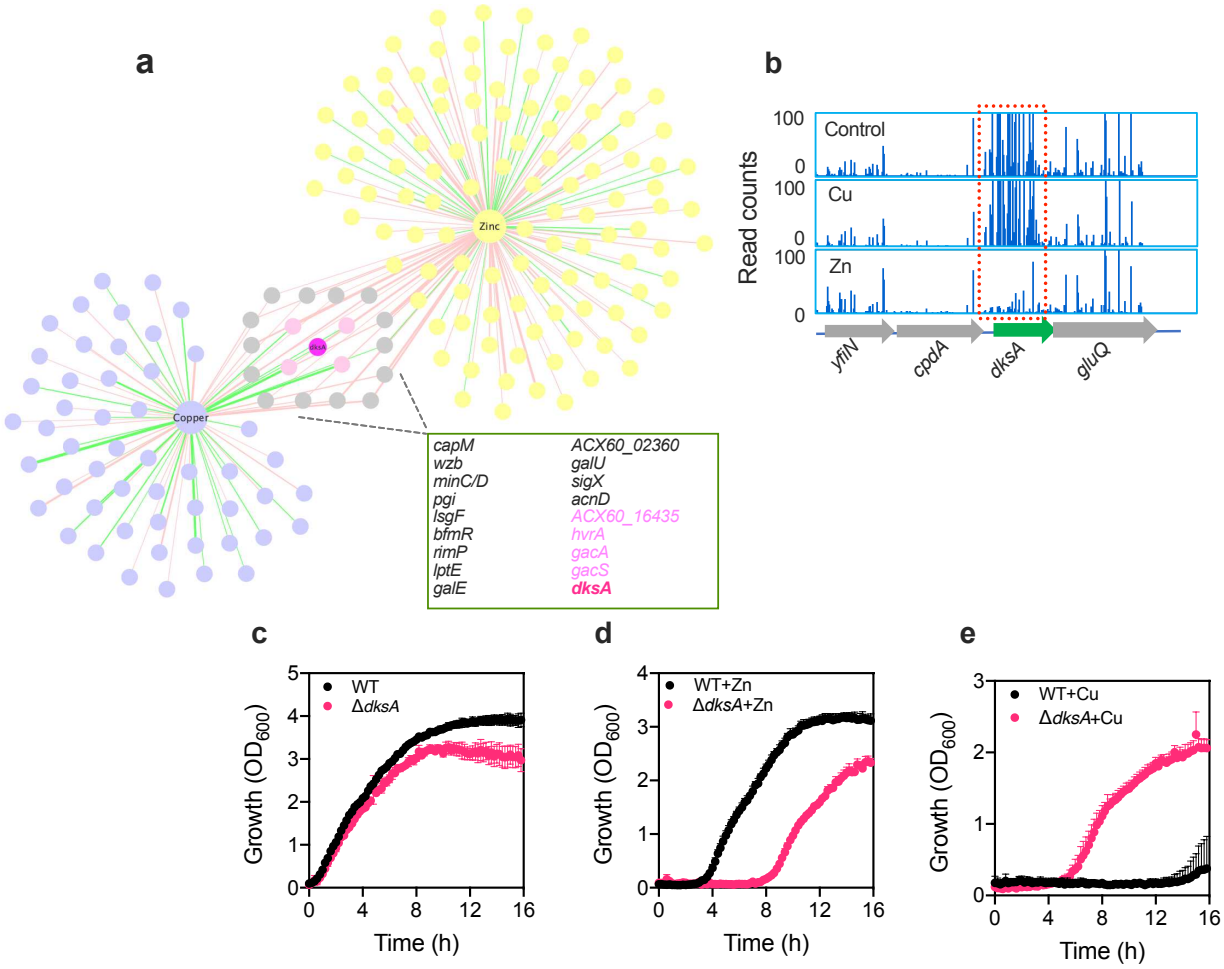

Figure 2. DksA has an opposite role in zinc and copper stress protection. (**a**) Network diagram showing the overlap of genes involved in tolerance and sensitivity to copper (purple) or zinc (yellow) stress. Genes represented by grey color are involved in tolerance to both copper and zinc. Pink colored genes have opposite effects under zinc and copper stresses with *dksA* in bold. The network analysis is based on 75 and 121 genes involved in copper and zinc stress with change in mutant abundance of >1.0 $\log_2$ fold change and $P_{adj} < 0.05$. An inset showing the list of 19 genes found detected in both copper and zinc. Gene with pink type have opposite effects. Cytoscape version 3.8.1. was used for network visualization [56]. (**b**) The TraDIS results showing the read counts in *dksA*; top (control), middle (6 mM $CuSO_4$) and bottom (3 mM $ZnSO_4$). The growth phenotype of wild-type and Δ*dksA* mutant in without stress (**c**) and in presence of 1.5 mM $ZnSO_4$ (**d**) and 5 mM $CuSO_4$ (**e**). Data are from at least three experiments, presented as mean (open black and peach circles ± StDev). See methods for detail.

The role of DksA in virulence and colonization in animal models

We first investigated the possible role that DksA plays in virulence for *A. baumannii* by employing a *Galleria mellonella* wax-moth insect model, which has been shown to be as an effective in vivo platform for molecular studies [57]. The initial *G. mellonella* infection assay was performed on two

200 different strains of *A. baumannii,* ATCC 17978 and AB5075_UW, and their respective Δ*dksA*
201 mutants as previously described [58]. We found that, for both *A. baumannii* strains, the Δ*dksA* mutants
202 killed significantly fewer larvae compared to wild-type, which killed all larvae within 3 days post-
203 infection (Fig. 3**a**). These promising results spurred us to investigate the role of DksA in a mammalian
204 host. For this, we intranasally challenged BALB/c mice with *A. baumannii* strain AB5075_UW or its
205 Δ*dksA* mutant derivative and after 24 h the mouse was sacrificed and organs were removed and
206 bacterial load counted. Strikingly, Δ*dksA* mutants could not be recovered from the blood of any mice
207 ($<10^2$ cells/mL), compared to $2.5x10^6$ cells/mL for wild-type (Fig. 3**b**). For all tissues, the *dksA*
208 mutant could still colonize, but not as well as the wild-type Fig. 3**c**-**g**), except for liver (Fig. 3**h**).
209 Recovery of the Δ*dksA* mutant from the respiratory tract (nose, bronchoalveolar and lung tissue), was
210 at least 2 orders of magnitude lower than that seen for wild-type cells (Fig. 3**c,d,e**).

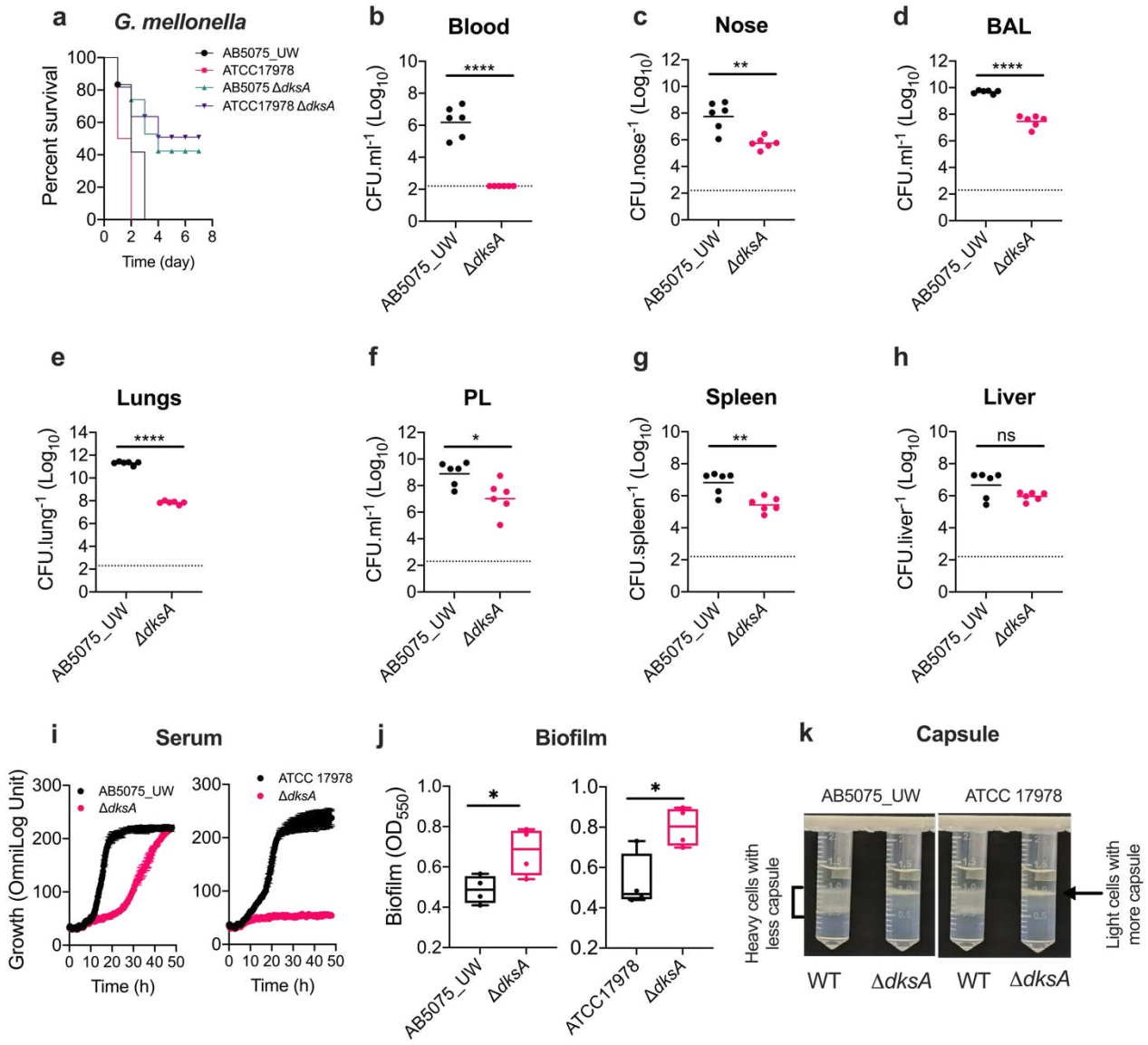

Figure 3. DksA-dependent virulence and niche specific colonization of *A. baumannii* and associated phenotype. (**a**) *Galleria mellonella* larvae were injected with 1×10^7 *A. baumannii* strains AB5075_UW or ATCC 17978 and their *dksA* deletion mutants. Survival of larvae was enumerated at every day post-challenge for six days. Enumeration of *A. baumannii* AB5075_UW and the *dksA* mutant in different host niches: blood (**b**), nasopharyngeal tissue (**c**), bronchioalveolar lavage, BAL (**d**), lung tissue (**e**), pleural cavity, PL (**f**), spleen tissue(g) and liver (**h**). Female Swiss mice were intranasally challenged with 2×10^8 CFU and colonization was examined 24 h post-challenge. Growth and respiration in presence of 50% human serum in LB (**i**), box and whiskers plots (min to max with all data points) showing estimates of crystal violet based biofilm (**j**) and density gradient qualitative estimation of capsule (**k**). See methods for detail. For each panel, the data represent the mean of at least two biological triplicates (±SEM). Statistical analyses were performed using a one-way ANOVA; * $p < 0.05$, ** $p < 0.01$, *** $p < 0.001$, **** $p < 0.0001$, and ns = not significant.

To understand the differences in the observed lack of ability of the *dksA* mutant to survive in the blood compared to other issues, we performed *in vitro* virulence assays on both *A. baumannii* strains (ATCC 17978 and AB5075_UW) and their *dksA* mutants. First, we tested the mutant's ability to propagate in human serum, which we found was greatly reduced for both Δ*dksA* mutant strains (Fig. 3**i**). Next, we tested the mutant's ability to form biofilm and capsule, and found that it was increased compared to wild-type (Fig. 3**j** and 3**k**). Taken together, these data show that DksA is needed for serum resistance and ultimately to infect the bloodstream but seems to repress other virulence determinants, like biofilm and capsule formation. We speculate that the increase in biofilm density resulting from *dksA* loss is what allows this mutant to still partially colonize tissue.

DksA acts as a global transcriptional regulator in *A. baumannii*

To identify the molecular mechanism underlying the divergent role of DksA in stress protection and virulence in *A. baumannii*, we conducted RNA-sequencing (RNAseq) on the ATCC 17978 Δ*dksA* mutant and wild-type with and without a shock treatment with copper or zinc. We used the same concentration of copper and zinc in both TraDIS and transcriptomic assays (Fig S1). For Δ*dksA* compared to wild-type without treatment, differential expression of 12.1% (461) of the total genes in the ATCC 17978 genome was observed (using a cut-off of $\log_2$FC >1.5 change and P_{adj}<0.05, Supplementary Table 2). Under copper and zinc stress, this increased so that the expression of ~1/5 of all genes (20.0% and 18.4% respectively) in Δ*dksA* were significantly altered, compared to treated wild-type.

To obtain a functional overview of the genes with altered expression in the *dksA* mutant, we used the "Pathway Omics Dashboards Tool" in the MetaCyc database, based on gene ontology [59]. The cellular processes of translation, respiration, ATP synthesis, amino acid synthesis, aromatic compound degradation, co-factor synthesis, nucleoside and nucleotide synthesis and oxidative stress protection

were amongst the most highly impacted, suggesting a crucial role of DksA regulation in both stress protection and metabolism (Supplementary Fig. 4). Individual genes and operons likely to be switched on or off under stress included genes known to be responsible for *A. baumannii* metal efflux and biofilm formation (e.g. *csuA/BABCDE*) (Supplementary Table 2). We found that the *csuA/BABCDE* operon was significantly upregulated (3.8 to 7.1-fold) in the Δ*dksA* strain. The *csu* operon encodes a pilus synthesis and assembly system required for initial bacterial attachment and biofilm formation [60, 61], consistent with our observation of higher biofilm formation in the Δ*dksA* mutant in both ATCC 17968 and AB5075_UW backgrounds (Fig. 3**j**).

Characterizing DksA-dependent induction of a stringent stress response

The stringent response in bacteria is primarily characterized by a down-regulation of translational machinery; ribosomal proteins (r-proteins) and ribosomal RNAs (rRNAs) [18, 19]. Therefore, to investigate the DksA-dependent stringent response in *A. baumannii*, we used transcription of r-protein genes as a proxy for the stringent response.

In *E. coli*, DksA disrupts the interaction of RNA polymerase (RNAP) with DNA by directly binding to RNAP, decreasing the transcription of rRNAs and r-proteins; thus a strain lacking DksA constitutively expresses rRNAs and r-proteins throughout different growth phases [18, 20, 62]. Consistent with this, we observed that the expression of r-proteins was increased in the Δ*dksA A. baumannii* cells compared to wild-type with the exception of *rpmE2* (give a range of FCs; Fig. 4**a**, top panel). *rpmE2* encodes an alternative ribosome sub-unit of 50S protein L31 (C- form), uniquely lacking a zinc binding motif. Under copper stress the expression of r-protein genes in the Δ*dksA* cells was also increased (log_2FC 1.5 to 3.7), whereas in wild-type cells subjected to copper stress they were mostly down regulated (Fig. 4**a**, middle panel). However, under zinc stress the transcription of r-protein genes was relatively unaffected in both wild-type and Δ*dksA* (Fig. 4**a**, bottom panel) besides *rpmE2*.

Both DksA and the C- form of RpmE (RpmE2) were previously found to be important for zinc homeostasis in *P. aeruginosa* [63]. Together, these results suggest that copper stress induces the stringent response in a DksA-dependent manner whereas zinc stress does not induce stringent response, potentially due to a zinc finger-dependent interaction with r-proteins.

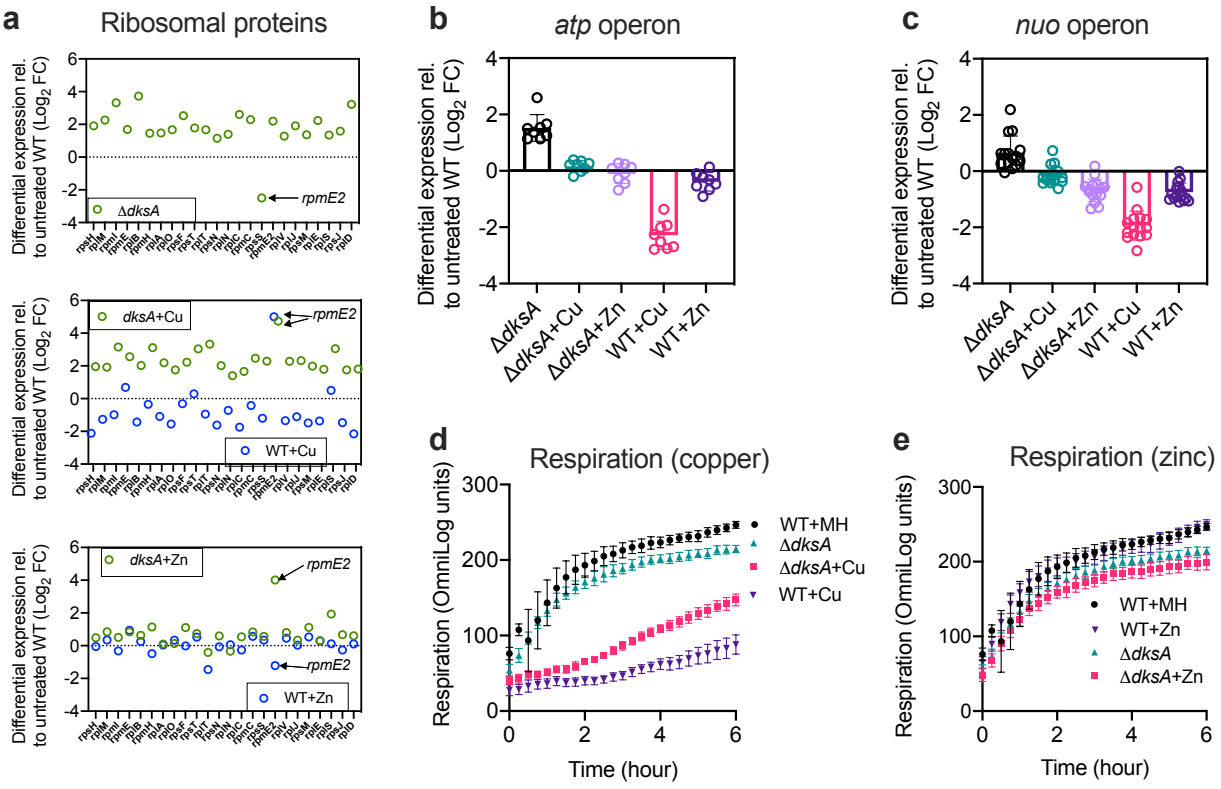

Figure 4. Copper stress attenuates expression of ribosomal protein and respiratory genes in *A. baumannii* in a DksA dependent manner. Differential expression (relative to untreated wild type) of genes involved in the synthesis of ribosomal proteins in Δ*dksA* mutant (**a**, top panel), wild-type and Δ*dksA* in presence of copper stress (**a**, middle panel) and wild-type and Δ*dksA* in presence of zinc stress (**a**, bottom panel), genes involved in ATP synthesis *atpIBEFHAGDC* operon (**b**) and NADH:quinone oxidoreductase and cytochrome bd-I ubiquinol oxidase subunits are encoded by *nuoABCEFGHIJKLMN and cydAB* operons (**c**). Effect of copper and zinc stress on respiration of wild-type ATCC 17978 and Δ*dksA* in present of copper (**d**) and zinc (**e**). Respiration activity data are from at five independent experiments, presented as mean ± StDev. See materials and method for detail.

The transcription of rRNA and r-proteins is highly correlated with the cellular concentration of initiating nucleotide triphosphates, ATP and GTP [64-66]. Therefore the divergent regulation of r-protein

genes under copper and zinc stresses by DksA could be due to differences in the cellular energy status under these two stresses. Most microorganisms use a branched electron transport chain composed of NADH-quinone oxidoreductases and quinol oxidases to efficiently couple electron exchange for ATP production by the F1F0 ATPase during aerobic respiration [67, 68]. In *A. baumannii*, enzymes necessary for ATP synthesis are encoded by the *atpIBEFHAGDC* operon whereas NADH:quinone oxidoreductase and cytochrome bd-I ubiquinol oxidase subunits are encoded by *nuoABCEFGHIJKLMN* and *cydAB* operons respectively. For the *dksA* mutant without treatment, the expression of many of the genes (9 out of 24, $\log_2$FC>1.5 and P_{adj}<0.05) in these operons were increased (2.4 – 6.1-fold), whereas expression remained largely (0/24 genes, $\log_2$FC>1.5 and P_{adj}<0.05) unaffected under both copper and zinc stresses (Fig. 4**b** and 4**c**). In wild-type *A. baumannii* under copper stress, expression of both the *atp* and *nuo/cyd* operons genes (22 out 24, $\log_2$FC>1.5 and P_{adj}<0.05) were decreased up to 7-fold, but were largely unaffected under zinc stress (Fig. 4**b** and 4**c**).

To test whether DksA impacts on respiration, we directly assayed respiration activities in wild-type and Δ*dksA* with and without copper and zinc stress using a tetrazolium redox based assay (Fig. 4**d**). Both wild-type and Δ*dksA* exhibited similar levels of respiratory activities under zinc stress, which were also indistinguishable from the untreated controls (Fig. 4**d)**. In contrast, copper stress resulted in a drastic reduction in respiration for wild-type cells. A reduction of respiratory activity was also noted in the Δ*dksA* strain under copper stress, but the effect was not as severe as in wild type, suggesting that copper stress inhibits respiration in *A. baumannii* and DksA plays a role in exacerbating this effect under copper stress. Collectively, these observations indicate that a decoupling of electron exchange in the respiratory system and subsequent reduction of ATP production may contribute to induction of the stringent response under copper stress.

DksA controls transcription of aromatic compound catabolism pathways

A. baumannii are metabolically versatile and can efficiently catabolize a large number of aromatic and aliphatic compounds [69]. In particular, aromatic degradation pathways are known to be important for *A. baumannii* virulence [11]. Most bacteria use the phenylacetate and β-ketoadipate pathways to metabolize aromatic compounds (Fig. 5**a**). A variety of aromatic compounds such as catechol and protocatechuate, can be degraded via these two pathways and are widely distributed among soil microorganisms [70, 71]. In the phenylacetate pathway, aromatic compounds are broken down into succinyl-CoA, whereas the β-ketoadipate pathway generates succinyl-CoA and acetyl-CoA before entering into TCA-glyoxylate cycle (Fig. 5**a**) [71].

We noted that the phenylacetate and β-ketoadipate pathways encoded by genes in *paa* (*paaNABCDEFGHK*) and *pca* (*pcaIJFBDKCHG*) operons respectively were the two most enriched pathways detected in our analysis of transcription in Δ*dksA* (Fig. 5**b** and 5**c**) but displayed specific induction conditions. The expression of genes in the *paa* operon decreased (between 12-330-fold) in Δ*dksA* cells in both the presence and absence of copper stress (Fig. 5**b**) and was decreased up to 8-fold under zinc stress. By contrast, when wild-type cells are treated with copper, expression of these genes was increased (5 to 14-fold; Fig. 5**b**). The effect of copper stress on expression of *pca* operon in wild-type strain was found to be similar to the *paa* operon, as it also increased relative to untreated cells (28 to 180-fold; Fig. 5**c**). When we gather all genes belonging to aromatic compounds together, it is clear that DksA acts as a transcriptional switch for regulating secondary gluconeogenic pathways (Fig. 5**d**).

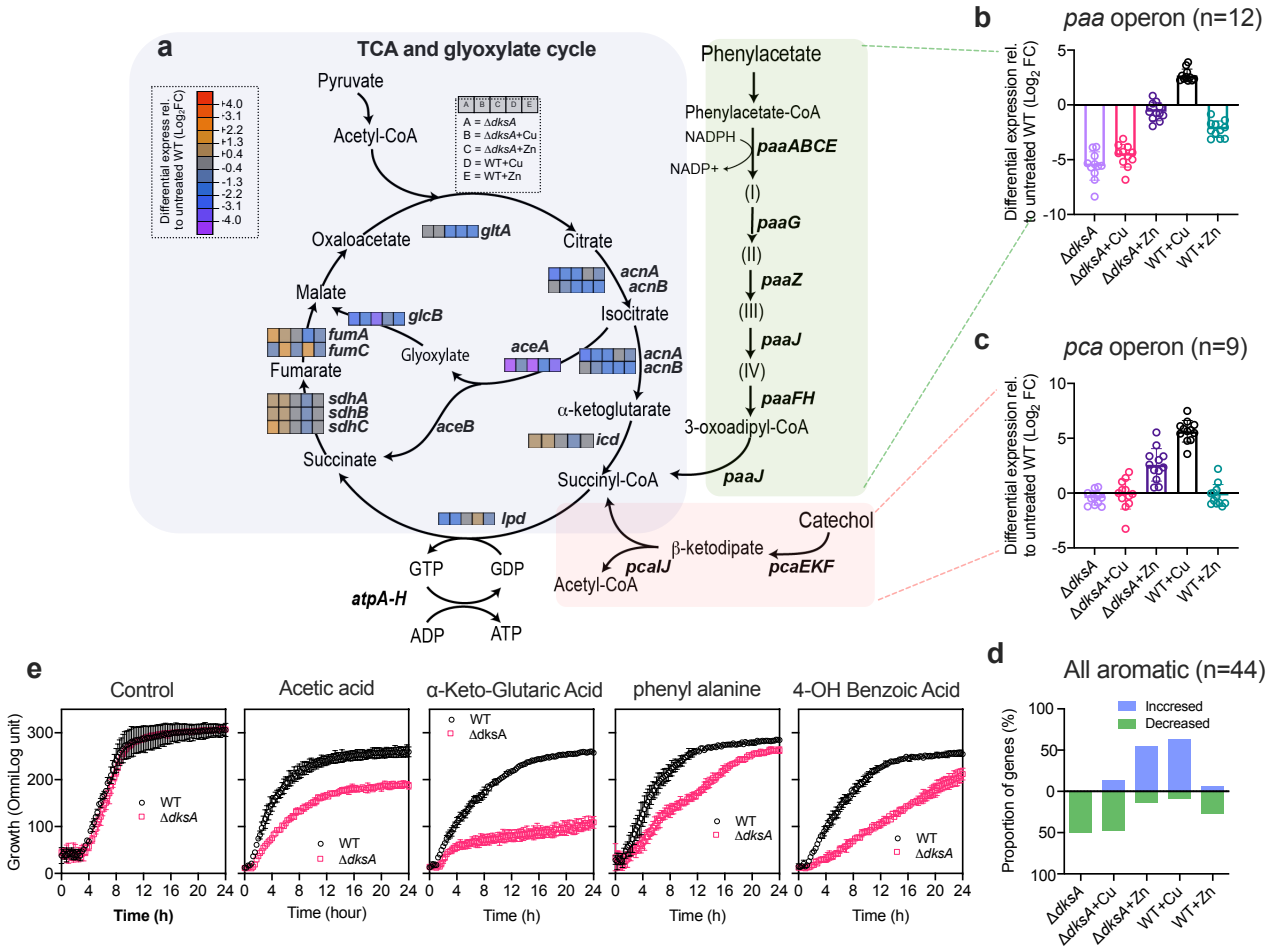

Figure 5. DksA regulates phenylacetate, β-ketoadipate and TCA-glyoxylate pathways in *A. baumannii*. **a**, Reactions and intermediates of the TCA and glyoxylate cycle (purple), phenylacetate (light green) and β-ketodipate pathways are based on BioCyc *A. baumannii* ATCC 17978 database [72]. Genes (enzymes) *paaABCE* (1,2-phenylacetyl-CoA epoxidase); *paaG*, (1,2-epoxyphenylacetyl-CoA isomerase); *paaZ* (oxepin-CoA hydrolase); *paaJ*, 3-oxoadipyl-CoA; *paaF*, 2,3-dehydroadipyl-CoA hydratase; *paaH* (3-hydroxyadipyl-CoA dehydrogenase). Intermediate products: (I) phenylacetyl-CoA; (II) 1,2-epoxyphenylacetyl-CoA; (III) 2-oxepin-2(3H)-yli-deneacetyl-CoA; (IV) 2,3-dehydroadipyl-CoA. Expression of 13-gene *paa* operon for phenylacetate (**b**) and *pca* operon for catechol catabolism (**c**) are based on transcriptomic data (Supplementary Table 2) relative to untreated wild-type (WT). **d**, Visualization of transcriptomics data in the aromatic compound degradation pathways (n=44 genes). Bars above the line (blue) represent percentages of genes increased and bars below the line (green) represent percentages of genes inhibited under given conditions. **e**, Strengths of aliphatic and aromatic compound utilization phenotypes of WT and its Δ*dksA* mutant were determined using Biolog Phenotype Microarray plates PM1 and PM2. The maximal kinetic curve was based on expressed OmniLog units (y-axis) over time. Metabolite utilization activity data are from two independent experiments, presented as mean ± StDev.

Previously, it has been proposed that the GacS/GacA two-component system operates as a switch between primary and gluconeogenic secondary metabolites in number of bacteria [73], and also aliphatic carboxylic acids such as acetate and propionate have been shown to be an environmental cue for the GacS/A system [74, 75]. In *A. baumannii gacS* is essential for the expression of *paa* operon [11]. In line with the reduced expression of the *paa* operon, expression of *gacA* was decreased 3.7-fold in the Δ*dksA* mutant in both the presence and absence of copper. In ATCC 17978 wild-type, expression of *gacA* remained unaffected in both copper and zinc stress conditions. Based on these observations, we conclude that DksA is required for the GacS/GacA-dependent metabolic switch during stress.

DksA controls the glyoxylate shunt in *A. baumannii*

Growth on aromatic compounds, acetate, or fatty acids also requires the activation of the glyoxylate shunt in the tricarboxylic acid cycle (TCA) and gluconeogenesis pathways[76]. More importantly, the glyoxylate shunt that bypasses the NADH producing steps is required within the electron transport chain for the production of ATP and plays important roles in oxidative stress, antibiotic resistance and pathogenesis [77-79]. In Δ*dksA* cells, two important genes responsible for the glyoxylate shunt, *aceA* encoding isocitrate lyase and *glcB* encoding malate synthase were reduced in expression by 18- and 5-fold respectively (Fig. 5**a**, Supplementary Table 2). When treated with zinc, expression of only *aceA* (18-fold) was decreased in Δ*dksA,* whereas this pathway was not affected under copper stress in both wild-type and Δ*dksA* strains (Fig. 5**a**). Thus, this data further demonstrates a DksA-dependent metabolic switch under metal stresses.

To test whether DksA is functionally important for catabolism of substrates associated with the glyoxylate shunt, we used phenotypic arrays with carbon-assay plates (Biolog MicroArrays PM1 and PM2) as described previously [69, 80]. With rich medium as a control, the Δ*dksA* mutant displayed respiratory curve similar to the wild type (Fig. 5**e**). As expected, the Δ*dksA* mutant showed growth

386 defects in media requiring a functional glyoxylate shunt, such as acetic and ketoglutaric acid (Fig.
387 5**e**). Similarly, we found that the Δ*dksA* mutant had a significant growth defect on a number of
388 aromatic carbon sources requiring the *paa* and *pca* operons including phenylalanine and 4-hydroxy
389 benzoic acid (Fig. 5**e**). Taken together, our transcriptomic and phenotypic data indicate that DksA
390 controls pathways associated with aromatic and aliphatic compounds.
391
392 **DksA acts as a general stress regulator by promoting tolerance of oxidative, osmotic stress and**
393 **antibiotic resistance in *A. baumannii***
394 *A. baumannii* and other Gram-negative bacteria contain an elaborate oxidative stress response system,
395 involved in detoxification of oxidizing agents such as hydrogen peroxide. This stress response is
396 characterized by the up-regulation of a number of genes, including catalase (*katG* and *katE*) and
397 NADH dehydrogenase/alkyl hydroperoxide reductase (*ahpC*, *ahpF1* and *ahpF2*), superoxide
398 dismutase (*sodC* and *sodB*), glutathione peroxidase (*btuE*) and universal stress protein A (*uspA*) genes
399 [81, 82]. In the *dksA* mutant, transcription of *katE*, *katG*, *sodC*, *btuE* and *uspA* was decreased compared
400 to wild-type (3.1 to 12.2-fold; Supplementary Fig. 5**a**), suggesting that DksA positively controls this
401 oxidative stress response system. To test whether DksA protects cells from oxidative damage, we
402 conducted phenotypic growth assays of wild-type and Δ*dksA* strains in the presence of exogenous
403 H_2O_2. As expected, the Δ*dksA* mutant was highly sensitive to oxidative stress (Supplementary Fig.
404 5**b**). In *E. coli*, expression of *katE* and *sodC* is regulated by RpoS [83] while in *A. baumannii* DksA
405 controls the expression of these genes. Other well-known stress response genes that are RpoS-
406 dependent in *E. coli* but controlled by DksA in *A. baumannii* included the trehalose synthesis genes
407 *otsA* (7.9-fold) and *otsB* (36-fold) required for cold and osmotic stress protection and infection [84].
408 Interestingly, in *E. coli* Δ*dksA* mutant the expression of the RpoS-dependent stress response genes
409 *katE*, *sodC*, *otsA* and *otsB* was not affected[85]. These results indicate that DksA has taken over the
410 functions of RpoS in *A. baumannii,* for at least some stress response genes.

Various stresses including antibiotics are known to perturb cellular respiration impacting redox homeostasis in cells [68, 86-88]. In addition, bacteria that unable to activate the stringent response generally show a decrease in antibiotic tolerance [89], and we found that the *dksA* mutant displayed reduced expression of genes involved in antibiotic efflux (Supplementary Fig. 5**c**). We therefore set out to investigate whether cells lacking DksA also displayed decreased resistance to antibiotics. The minimum inhibitory concentration (MIC) was determined for nine different antibiotics representing the four major classes for 3 wild-type strains and their respective Δ*dksA* mutants: a multidrug resistant *A. baumannii* strain (AB5075_UW), a more sensitive laboratory strain (ATCC 17978) and the sensitive *E. coli* K-12 strain harboring *rpoS* as a control. We found that despite having very different antibiotic resistance profiles, both *A. baumannii* strains exhibited a very similar effect for *dksA* disruption of reduction in antibiotic resistance. Four out of nine (or 44%) antibiotics tested had a decreased MIC (2 to 16-fold) in the Δ*dksA* mutant of AB5075_UW and six out of nine (67%) in ATCC 17978 (Supplementary Fig. 5**d**). However, in the *E. coli* Δ*dksA* strain, we noted that although six antibiotics (67%) had a decreased MIC, the MIC for 2 antibiotics (amikacin and rifampicin) increased by 2 to 4-fold (Supplementary Fig. 5**d**). Taken together, this data shows that DksA plays a major role in controlling the central metabolism of *A. baumannii*. Interestingly, its disruption leads to increased sensitivity to different classes of antibiotics, but in a sensitive, RpoS-containing strain of *E. coli* these DksA-related antibiotic resistance effects are divergent.

Concluding remarks

Our systematic genomics-based approach has helped to unravel the intricate details of how DksA controls stress responses and virulence in *A. baumannii*, an important pathogen lacking the global stress regulator RpoS [9, 35]. Our results suggest that activity of DksA may be involved in numerous

stress conditions, as summarised in Fig. 6. The overall strategy of *A. baumannii* in employing DksA for many activities that are RpoS-controlled in other pathogens can be rationalized in terms of its adaptive advantages. While RpoS positively regulates many gene required for stress protection, it also adversely effects the utilisation of secondary carbon sources such as acetate and succinate [90]. In *A. baumannii*, our results show that DksA plays unique roles by regulating RpoS-dependent stress genes without exerting notable trade-offs associated with metabolism of such secondary carbon sources.

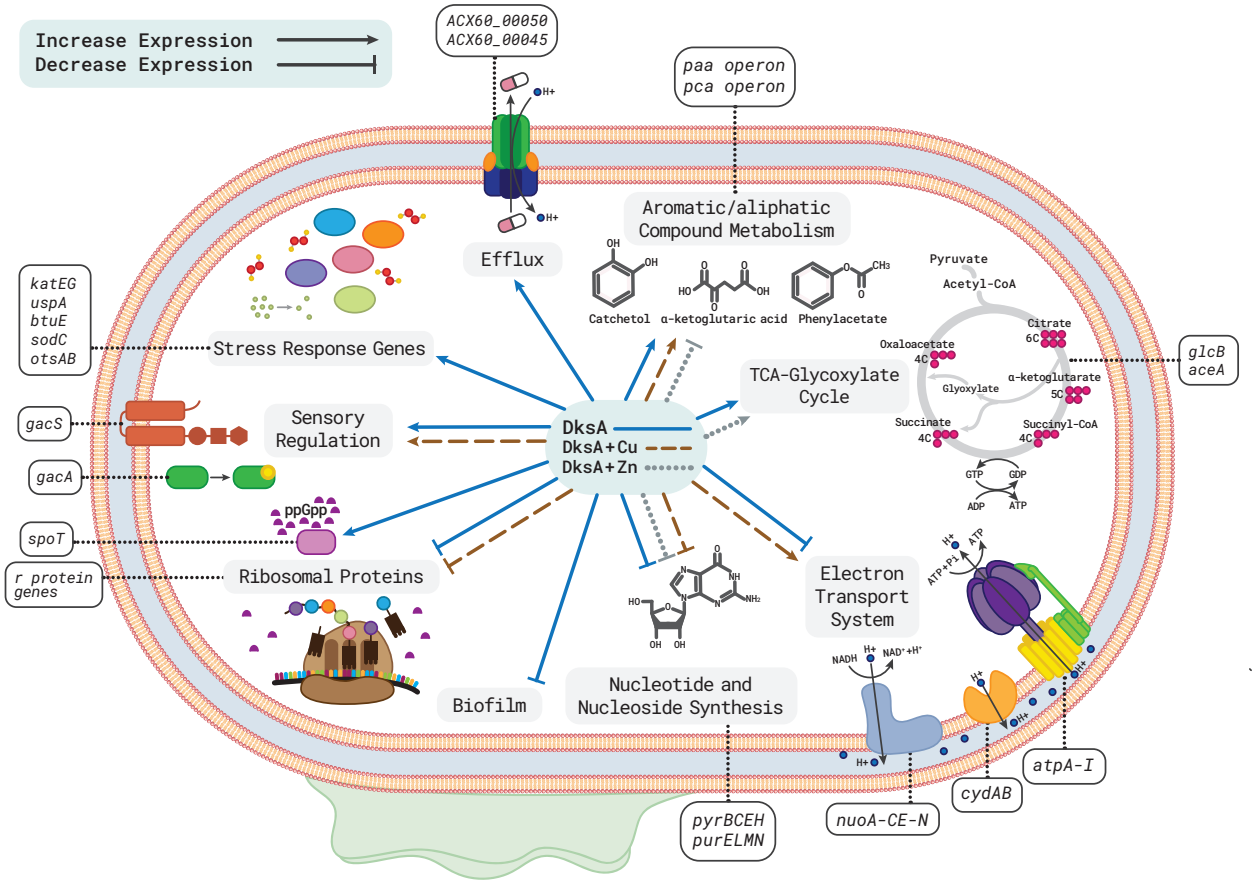

Figure 6. An overview of DksA-dependent stress regulation in *A. baumannii*. The model depicting the various pathways and their cellular locations and regulatory roles of DksA are illustrated with arrows (activation) and blunt ended lines (inhibition) from the green centre. The illustration is based on the gene expression in *A. baumannii* ATCC 17978 Δ*dksA* mutant in presence of $ZnSO_4$ (3

mM, dotted grey line) or $CuSO_4$ (6 mM, dashed red line) and absence of either metal stresses (solid blue line), and are discussed in text.

Since DksA is a substrate of the ATP-dependent ClpXP protease [91], environmental conditions affecting ATP synthesis may influence the activity of DksA. This is already evident from the observed switching role of DksA in copper and zinc stresses. Some of the pleiotropic effects of DksA can thus be explained. For instance, copper stress suppressing transcription of r-proteins, a hallmark of the stringent response, is most likely due to mismetallation of other metals in proteins involved in the electron transport system needed for aerobic respiration and ATP production. Copper is known to displace Fe directly from 4Fe-4S iron-sulfur clusters in proteins requiring this prosthetic group[92]. The reduction of ATP synthesis and hence ClpXP protease activity might increase the activity of DksA under copper stress leading to increase in expression of DksA-dependent metabolic genes such as *paa* and *pca* operons. Conversely, the inability to activate the stringent response in strain lacking DksA might have led to increase sensitivity to variety of stresses including the heavy metal zinc. Since antibiotics efficacy is determined by cellular metabolic states [87, 89], the broad effect of DksA on antibiotic sensitivity (Supplementary Fig. 5d) may stem from its effects on central metabolism.

The positive role of DksA in metabolic pathways requiring catabolism of secondary (gluconeogenic) carbon sources (e.g. acetate and other aliphatic and aromatic compounds), which could be primary carbon and energy sources in natural or host environments might have contributed to the observed attenuation of *A. baumannii* virulence in *G. mellonella* and mouse models. Although DksA-dependent activation of aliphatic and aromatic acids catabolic pathways is essential for efficient utilization of secondary carbon source catabolism and necessary for virulence *in vivo*, it is deleterious in laboratory environment under Cu stress.

Our study lays the groundwork for understanding just how important DksA is in general *A. baumannii* stress response, antibiotic resistance and virulence. However, further investigation into the specifics of DksA function, for example whether activity and/or concentration of DksA varies with environmental conditions or the precise mechanism through which DksA works to alter antibiotic resistance differently between bacterial strains, is warranted. In conclusion, our analysis provides a detailed insight into the unique role that DksA plays in stress protection, metabolism and virulence in this deadly pathogen and reveals a newly found alternative to the better-known sigma factor dependent resistance mechanisms. Our study reiterates the need for assessing gene function in specific bacterial species and not simply transferring function based on homology. The identification of RpoS-independent general stress response provides a novel approach of bacterial adaptative strategies, and it will be very interesting to explore whether DksA plays a similar role in other bacterial species lacking RpoS, or whether there are further novel strategies for regulating general stress responses.

Materials and Methods

Bacteria strains, media and growth conditions

The wild-type *A. baumannii* strains used were ATCC 17978 (NCBI accession number: CP012004.1) and AB5075_UW (NCBI accession number: CP008706.1). The Tn*26* insertion mutant derivatives of AB5075_UW were purchased from the Manoil Laboratory [53] and used for individual growth assays to validate TraDIS results. A total of 28 mutants was used for the individual growth assays. The *dksA*::kan mutant derivative of ATCC 17978 was constructed for this study using the previously published protocol [93, 94]. To confirm that both the ATCC 17978 and AB5075_UW *dksA* mutants contained no secondary mutations, we whole genome sequenced each mutant (>20 x coverage on an Illumina MiSeq platform) and employed the Snippy pipeline version 4.3.6 for mutation single

nucleotide polymorphism (SNP) identification [95]. All primers used in this study are listed in Supplementary Table 3.

For routine overnight culturing of *A. baumannii* strains, a single colony from cation adjusted Mueller Hinton (MH) agar (for AB5075 low switching opaque type was chosen to minimise phase variation) was used to inoculate 5 mL of MH broth medium.

Construction of transposon mutant library

The ATCC 17978 *A. baumannii* dense transposon library used in this study was constructed using the protocol as previously described [49]. Briefly, transposomes were prepared by using EZ-Tn*5* transposase (Epicentre Biotechnology) and a custom Tn*5* transposon carrying a kanamycin resistance cassette amplified from the plasmid pUT_Km [96] using the primer set as described previously [97]. The transposomes (0.25 µL) were electroporated into 60 µL of freshly prepared electrocompetent cells using a Bio-Rad GenePulser II set to 1.8 kV, 25 µF, and 200 Ω in a 1-mm electrode gap (Bio-Rad). For preparation of electrocompetent cells, the 125 mL cultures were grown in 500 ml baffled flasks at 37°C in an Infor HT shaking incubator (Switzerland) at 200 rpm until they reached mid-log phase (OD_{600} = 0.5). The cultures were then place on ice for 15 min with occasional swirling before centrifugation for 10 min at 4ºC, washed twice with ice-cold 10% glycerol in MilliQ water. The washed electro-competent cells were then resuspended with 150 µl of ice-cold 10% glycerol. The cells were resuspended in 1 mL of SOC medium and incubated at 37ºC with shaking 200 rpm for 2 hours then spread on MH-agar supplemented with 7 µg/mL kanamycin (Sigma-Aldrich, Australia). Usually, 12 to 16 transformations were performed for each batch. Number of transformants in each batch ranged from 10,000 to 50,000. Approximately 250,000 mutants were collected from a total of 10 batches and stored as glycerol stocks at -80ºC.

Transposon mutant library metal stress challenge and Transposon-directed insertion site sequencing (TraDIS) of mutant library

Approximately 10^9 viable mutant cells were inoculated into 10 ml MH broth and grown at 37°C for 8 hours with shaking (200 rpm). The culture (500 µL) containing approximately 10^9 cells was sub-cultured into 10 mL fresh MH broth with or without 6 mM $CuSO_4$ or 3 mM $ZnSO_4$ in duplicate and grown for 16 hours at 37°C with shaking (200 rpm). Genomic DNA was then extracted from approximately 10^10 cells using the DNeasy UltraClean Microbial Kit (Qiagen) according to the manufacturer's protocol. Sequencing and analysis of transposon mutant library were performed using the transposon-directed insertion site sequencing (TraDIS) as described previously [49, 50]. The primer sets used for PCR amplification of TraDIS fragments and sequencing were described previously [97]. Samples were sequenced on a HiSeq2500 Illumina sequencing platform at the Wellcome Sanger Institute, generating approximately 2 million 50 bp single-end reads per sample as previously described. TraDIS sequence reads were deposited in the European Nucleotide Archive under accession number ERP118051 and analysed using the BioTraDIS pipeline with default parameters as described in [50]. The final ATCC 17978 Tn*5* library density was >110,000 unique mutants.

Time kill assay for the selection of copper and zinc concentrations for mutant library challenge

In order to identify sub-inhibitory concentration of $CuSO_4$ and $ZnSO_4$ for treatment of Tn*5* transposon library we performed time kill assays. Approximately 10^9 cells from overnight culture of ATCC 17978 was sub-cultured into fresh 10 mL MH broth spiked with different amount of $CuSO_4$ (0, 3, 6, 8, 16 and 24 mM final concentration) or $ZnSO_4$ (0, 3, 4, 8, 16, and 24 mM final concentration) and incubated at 37°C with shaking. At 0, 1, 2, 4, 5 and 24 h time points, 100 µL samples were taken, 10-fold serially diluted in sterile PBS and 10 µL of each dilution was then spotted on MH-agar plates. Plates were incubated at 37°C overnight and colonies were enumerated to determine the surviving cells.

547

548 **Transcriptomic Analyses**

549 Three independent *A. baumannii* strain ATCC 17978 and its Δ*dksA* mutant were grown overnight in
550 5 ml MH broth with shaking 200 rpm at 37°C. The overnight cultures were diluted 200-fold in fresh
551 MH medium and grown to mid-log phase (OD600 of 0.55). Each culture was divided into three flasks,
552 two cultures were treated with either 6 mM $CuSO_4$ or 3 mM $ZnSO_4$ and one left untreated as control
553 and grown for 40 mins. RNA extraction was carried out using the miRNeasy mini kit (Qiagen) and
554 DNA was eliminated using the TURBO DNA-free kit (Ambion Inc., USA), as per manufacturer's
555 instructions. Libraries were constructed using Universal Prokaryotic RNA-Seq Library preparation
556 kit (Tecan, USA) according to the manufacturer protocol. The samples were sequenced on Novaseq
557 Illumina platform, producing, ~3 million 150 bp paired-end reads per sample ~ 25 Gbp of data in
558 total. The raw sequencing data was deposited under GEO accession number GSE169081. Reads were
559 quality controlled using FastQC and trimmed using bbduk (v38.79) with the included adapters.fa file
560 and parameters ktrim=r k=23 mink=11 hdist=1 qtrim2=t trimq=10 tpe tbo. Reads were then mapped
561 using bbmap (v38.79) with parameters k=13 and ambig=toss against the Acinetobacter baumannii
562 genome (accession CP000522) and plasmids (accessions CP000523, CP012004, CP012005), sorted
563 using samtools (v1.6), and quantified using HTSeq (v0.12.4) with default parameters. Read counts
564 were aggregated using a custom perl script and used as the basis for differential expression analysis.
565 Differential expression analysis was performed in the R language, using the edgeR package (v3.30.3)
566 using the quasi-likelihood fit and test functions (glmQLFit, glmQLFTest). Genes differentially
567 expressed, as defined by >3-fold change and P_{adj} <0.05, are listed in Supplementary Table 2. The
568 function of genes in *A. baumannii* were allocated using eggNOG-mapper, and the resulting GO terms
569 and KEGG pathways were used for gene set enrichment analysis (GSEA) using Fry, a fast
570 approximation of the ROAST gene set test included in the edgeR package.

571

For visualisation metabolic pathways in our RNA sequencing data we also used combined of the EcoCyc [98] and MetaCyc [59] database in Omics Dashboard Tool. Information in Dataset S1 was imported into an EcoCyc (ecocyc.org) analyzed using the Omics Dashboard. Enrichment or depletion of metabolic pathways then analysed using the Fisher's exact test hypothesis and significant values of <0.05. Enrichment or depletion scores ($-\log_{10}$ P values) for each pathway in the dashboard were downloaded, and figures were then created using PRISM graphing software (Graph-Pad Software Inc). We also downloaded tables showing list of genes from the dashboard and were used to calculate the percentage of transcripts that increased or decreased, as shown in Fig. 5**d**. We could not map 1338 gene out of 2470 significant up or downregulated in at least one condition due to lack of their functional annotation.

Animal infection experiments

The *Galleria mellonella* infection experiments, larvae were performed as previously described in [58]. Briefly, triplicate assays of 5 larvae (200-230mg) were injected with 1×10^7 *A. baumannii* strains AB5075_UW or ATCC 17978 and their *dksA* deletion mutants. Survival and health of larvae were enumerated at every day post-challenge for six days according to the *G. mellonella* Health Index Scoring System [99].

A mice *in vivo* model was used for enumeration of *A. baumannii* AB5075_UW and the *dksA* mutant in different host niches: blood, nasopharyngeal tissue, bronchioalveolar lavage, BAL, lung tissue, pleural cavity, PL, spleen tissue and liver. Female Swiss mice were intranasally challenged with 2×10^8 CFU and colonization was examined 24 h post-challenge as previously described.

Growth phenotypic assays

For all growth phenotypic assays a single colony from Luria Bertani (LB) agar plates was used to inoculate 5 mL of LB broth medium. Overnight cultures were diluted to an optical density at 600 nm (OD_{600}) of 0.01 in 105 µl LB broth with or without stress treatments in 96-well plates. We supplemented $ZnSO_4$ (1.5 mM), $CuSO_4$ (3 mM or 5 mM) and H_2O_2 (0.5 mM) in LB medium for zinc, copper and oxidative stresses respectively. For all growth assays, cultures were incubated at 37 °C for 16 h with shaking at 200 rpm in a PHERAstar FS Spectrophotometer (BMG Labtech). Cell growth was monitored at 0.1 h intervals by measuring OD_{600}. Growth curves were used to calculate area under curve (AUC) using Graphpad Prism 9.0. The difference in AUC between wild-type and mutants was and then used as a proxy for fitness under different stress conditions.

Biolog phenotypic microarray

The phenomes of *A. baumannii* ATCC 17978 its Δ*dksA* mutant were assayed with the Biolog Phenotype MicroArrayTM (PM) system [80] to identify compounds that could serve as sole carbon (PM1-2; 190 compounds). Additionally, sensitivities to stress conditions (PM9-10; 192 conditions) were also tested. All phenotypic tests were performed as per the manufacturer's protocol. Following inoculation, all PM plates were incubated in an OmniLog reader (Biolog) aerobically at 37°C for 48 h. Reduction of the tetrazolium-based dye (colourless) to formazan (violet) was monitored and recorded at 15 min intervals by an integrated charge-coupled device camera. The resultant data were analysed with the supplied manufacturer's software, resulting in a time-course curve for colorimetric change equating to respiration rate.

Respiration activity assay

For respiration assay, wild-type ATCC 17978 and Δ*dksA* mutant cells in 5 ml MH broth were grown to mid-log phase (OD600 = 0.5) at 37°C with shaking at 200 rpm and treated with 6 mM $CuSO_4$ or 3

mM $ZnSO_4$ for 40 mins, 1 ml cultures were centrifuged for 1.5 mins and resuspended with fresh MH medium containing 0.1% tetrazolium dye and chloramphenicol (200 µg/ml). Chloramphenicol was used to prevent further protein synthesis allowing us to capture respiration status during 40 mins of Cu or Zn treatment. 150 µL of cells were then transferred into 96-well culture plates. The plates were incubated in an OmniLog reader (Biolog) aerobically at 37°C for 6 h. Reduction of the tetrazolium-based dye (colourless) to formazan (violet) was monitored and recorded at 15 min intervals by an integrated charge-coupled device camera. The resultant data were analysed with the supplied manufacturer's software as in the Biolog phenotypic microarray assay.

Serum growth inhibition assay

For serum growth inhibition assay 10^5 CFU in 10 µL from exponentially growing cells in MH were transferred into 100 µL 50% serum in MH plus 0.1% tetrazolium dye in 96-well microplates. The plates were then incubated in an OmniLog reader (Biolog) aerobically at 37°C for 48 h. Reduction of the tetrazolium-based dye (colourless) to formazan (violet) was monitored and recorded at 15 min intervals by an integrated charge-coupled device camera. The resultant data were analysed with the supplied manufacturer's software.

Biofilm formation and capsule synthesis

For biofilm formation assay we used the previously published method [100]. Briefly, overnight cultures were diluted 100-fold in 100 µL LB broth in 96-well dish. Cells were then incubated for 24 h at 37°C without shaking. Bacterial cells were removed by pipetting washed three times with PBS to remove unattached cells, added 125 µl of a 0.1% crystal violet (CV) aqueous solution and incubated for 15 mins at room temperature. After rinsing 3 times with water and drying for 2 hours, 125 µL of 30% acetic acid in water was added to each well, incubated for 15 mins to allow complete solubilisation of CV and 125 µL of solubilised CV was transferred a new flat bottom microtiter plate. Biofilm

formations were then estimated by measuring absorbance in a plate at 550 nm using 30% acetic acid solution as blank.

For qualitative estimation of capsule levels, we used density gradient centrifugation as previously described [101], which is based on the effect of cell-associated capsule on bacterial density. Briefly, 1 ml of overnight grown cultures were centrifuged, washed with PBS and resuspended in 1 ml PBS. The OD_{600} of the cell suspensions was then adjusted to 1, translating approximately 8 x 10^8 cells/ml, and 400 µl of the cell suspensions were loaded gently on the top of a solution of 37.5% (AB5075) or 47.5% (ATCC17978) Percoll in PBS. A second layer of 60% Percoll was included to aid visualisation of the cells following centrifugation. The tubes containing biphasic percoll solution and cell suspension were centrifuged for 5 mins at 3000g.

Minimal inhibitory concentration (MIC) assay

The three wild type strains (*A. baumannii* AB5075 and ATCC 17978, and *E. coli* K-12) and their *dksA* single gene knockouts were streaked from frozen on an MH plate overnight at 37°C. A single colony was inoculated in 10 mL of MH in a 50 mL falcon tube and shaken at 200 rpm in 37°C until an OD_{600} of 0.5 was reached. Antibiotic two-fold dilutions were prepared in triplicate in 96-well plates to a volume of 140 µL using a multichannel pipette. A 1/400 dilution was made in PBS for each of the cultures once they had reached OD_{600} of 0.5. 15 µL of the culture dilutions was dispensed into each well, bringing the final volume to 155 µL. Each plate was covered with an AeraSeal™ film (Sigma Aldrich, cat. A9224-50EA) and incubated at 37°C for overnight with shaking (200 rpm). Plates were imaged at OD_{600} and MICs were reported at the lowest concentration where the majority of wells had 80% growth inhibition compared to the positive control.

Declarations

Acknowledgements

This work was supported by the National Health and Medical Research Council (Australia) through Project Grant 1159752 to BAE and AKC. AKC was supported by an Australian Research Council (ARC) DECRA fellowship (DE180100929).

Authors' contributions

AKC, RM, BAE, JP and ITP designed the study. RM, GS, FA, LB, ND, HD, LS and BAE performed the experiments and analyse data. RM, AKC, BAE, FA, ITP, LS and NND contributed to the drafting of the manuscript.

References:

1. Peleg, A.Y., Seifert, H. & Paterson, D.L. *Acinetobacter baumannii*: emergence of a successful pathogen. *Clin Microbiol Rev* **21**, 538-582 (2008).
2. Antunes, L.C., Visca, P. & Towner, K.J. *Acinetobacter baumannii*: evolution of a global pathogen. *Pathog Dis* **71**, 292-301 (2014).
3. WHO WHO publishes list of bacteria for which new antibiotics are urgently needed. *WHO Media centre* (2017).
4. Fang, F.C., Frawley, E.R., Tapscott, T. & Vazquez-Torres, A. Bacterial Stress Responses during Host Infection. *Cell Host Microbe* **20**, 133-143 (2016).
5. Gottesman, S. Stress Reduction, Bacterial Style. *J Bacteriol* **199** (2017).
6. Chin, C.Y. *et al.* A high-frequency phenotypic switch links bacterial virulence and environmental survival in Acinetobacter baumannii. *Nat Microbiol* **3**, 563-569 (2018).
7. Hood, M.I. & Skaar, E.P. Nutritional immunity: transition metals at the pathogen-host interface. *Nat Rev Microbiol* **10**, 525-537 (2012).
8. Juttukonda, L.J. *et al.* Acinetobacter baumannii OxyR Regulates the Transcriptional Response to Hydrogen Peroxide. *Infect Immun* **87** (2019).
9. Geisinger, E., Mortman, N.J., Vargas-Cuebas, G., Tai, A.K. & Isberg, R.R. A global regulatory system links virulence and antibiotic resistance to envelope homeostasis in Acinetobacter baumannii. *PLoS Pathog* **14**, e1007030 (2018).
10. Gebhardt, M.J. & Shuman, H.A. GigA and GigB are Master Regulators of Antibiotic Resistance, Stress Responses, and Virulence in *Acinetobacter baumannii*. *J Bacteriol* **199** (2017).
11. Cerqueira, G.M. *et al.* A global virulence regulator in *Acinetobacter baumannii* and its control of the phenylacetic acid catabolic pathway. *J Infect Dis* **210**, 46-55 (2014).
12. Hood, M.I. *et al.* Identification of an *Acinetobacter baumannii* zinc acquisition system that facilitates resistance to calprotectin-mediated zinc sequestration. *PLoS Pathog* **8**, e1003068 (2012).

13. Mihara, K. *et al.* Identification and transcriptional organization of a gene cluster involved in biosynthesis and transport of acinetobactin, a siderophore produced by *Acinetobacter baumannii* ATCC 19606T. *Microbiology (Reading)* **150**, 2587-2597 (2004).
14. Battesti, A., Majdalani, N. & Gottesman, S. The RpoS-mediated general stress response in Escherichia coli. *Annu Rev Microbiol* **65**, 189-213 (2011).
15. Hengge-Aronis, R. Signal transduction and regulatory mechanisms involved in control of the sigma(S) (RpoS) subunit of RNA polymerase. *Microbiol Mol Biol Rev* **66**, 373-395, table of contents (2002).
16. Weber, H., Polen, T., Heuveling, J., Wendisch, V.F. & Hengge, R. Genome-wide analysis of the general stress response network in *Escherichia coli:* sigmaS-dependent genes, promoters, and sigma factor selectivity. *J Bacteriol* **187**, 1591-1603 (2005).
17. Perederina, A. *et al.* Regulation through the secondary channel--structural framework for ppGpp-DksA synergism during transcription. *Cell* **118**, 297-309 (2004).
18. Gourse, R.L. *et al.* Transcriptional Responses to ppGpp and DksA. *Annu Rev Microbiol* **72**, 163-184 (2018).
19. Cashel, M., Gentry, D., Hernandez, V. & Vinella, D. The stringent response., in *Escherichia coli and Salmonella: Cellular and Molecular Biology*. (eds. F.C. Neidhardt *et al.*) 1458–1496. (American Society for Microbiology Press, pp. 1458–1496., Washington DC; 1996).
20. Paul, B.J. *et al.* DksA: a critical component of the transcription initiation machinery that potentiates the regulation of rRNA promoters by ppGpp and the initiating NTP. *Cell* **118**, 311-322 (2004).
21. Brown, L., Gentry, D., Elliott, T. & Cashel, M. DksA affects ppGpp induction of RpoS at a translational level. *J Bacteriol* **184**, 4455-4465 (2002).
22. Girard, M.E. *et al.* DksA and ppGpp Regulate the sigma(S) Stress Response by Activating Promoters for the Small RNA DsrA and the Anti-Adapter Protein IraP. *J Bacteriol* **200** (2018).
23. Webb, C., Moreno, M., Wilmes-Riesenberg, M., Curtiss, R., 3rd & Foster, J.W. Effects of DksA and ClpP protease on sigma S production and virulence in *Salmonella typhimurium*. *Mol Microbiol* **34**, 112-123 (1999).
24. Boyle, W.K. *et al.* DksA-dependent regulation of RpoS contributes to Borrelia burgdorferi tick-borne transmission and mammalian infectivity. *PLoS Pathog* **17**, e1009072 (2021).
25. Mogull, S.A., Runyen-Janecky, L.J., Hong, M. & Payne, S.M. dksA is required for intercellular spread of Shigella flexneri via an RpoS-independent mechanism. *Infect Immun* **69**, 5742-5751 (2001).
26. Tehranchi, A.K. *et al.* The transcription factor DksA prevents conflicts between DNA replication and transcription machinery. *Cell* **141**, 595-605 (2010).
27. Meddows, T.R., Savory, A.P., Grove, J.I., Moore, T. & Lloyd, R.G. RecN protein and transcription factor DksA combine to promote faithful recombinational repair of DNA double-strand breaks. *Mol Microbiol* **57**, 97-110 (2005).
28. Trautinger, B.W., Jaktaji, R.P., Rusakova, E. & Lloyd, R.G. RNA polymerase modulators and DNA repair activities resolve conflicts between DNA replication and transcription. *Mol Cell* **19**, 247-258 (2005).
29. Myka, K.K., Kusters, K., Washburn, R. & Gottesman, M.E. DksA-RNA polymerase interactions support new origin formation and DNA repair in *Escherichia coli*. *Mol Microbiol* **111**, 1382-1397 (2019).
30. Paul, B.J., Berkmen, M.B. & Gourse, R.L. DksA potentiates direct activation of amino acid promoters by ppGpp. *Proc Natl Acad Sci U S A* **102**, 7823-7828 (2005).
31. Ishii, Y. *et al.* Deletion of the yhhP gene results in filamentous cell morphology in *Escherichia coli*. *Biosci Biotechnol Biochem* **64**, 799-807 (2000).

32. Wang, J. *et al.* Transcriptional analysis reveals the critical role of RNA polymerase-binding transcription factor, DksA, in regulating multi-drug resistance of Escherichia coli. *Int J Antimicrob Agents* **52**, 63-69 (2018).
33. Henard, C.A., Bourret, T.J., Song, M. & Vazquez-Torres, A. Control of redox balance by the stringent response regulatory protein promotes antioxidant defenses of Salmonella. *J Biol Chem* **285**, 36785-36793 (2010).
34. Yun, J. *et al.* Role of the DksA-like protein in the pathogenesis and diverse metabolic activity of Campylobacter jejuni. *J Bacteriol* **190**, 4512-4520 (2008).
35. Robinson, A. *et al.* Essential biological processes of an emerging pathogen: DNA replication, transcription, and cell division in *Acinetobacter* spp. *Microbiol Mol Biol Rev* **74**, 273-297 (2010).
36. Begg, S.L. The role of metal ions in the virulence and viability of bacterial pathogens. *Biochem Soc Trans* **47**, 77-87 (2019).
37. Andreini, C., Bertini, I., Cavallaro, G., Holliday, G.L. & Thornton, J.M. Metal ions in biological catalysis: from enzyme databases to general principles. *J Biol Inorg Chem* **13**, 1205-1218 (2008).
38. Grass, G., Rensing, L. & Rensing, C. Metal toxicity. *Metallomics* **3**, 1095-1097 (2011).
39. Palmer, L.D. & Skaar, E.P. Transition Metals and Virulence in Bacteria. *Annu Rev Genet* **50**, 67-91 (2016).
40. Achard, M.E. *et al.* Copper redistribution in murine macrophages in response to Salmonella infection. *Biochem J* **444**, 51-57 (2012).
41. Guilhen, C., Taha, M.K. & Veyrier, F.J. Role of transition metal exporters in virulence: the example of Neisseria meningitidis. *Front Cell Infect Microbiol* **3**, 102 (2013).
42. Djoko, K.Y., Ong, C.L., Walker, M.J. & McEwan, A.G. The Role of Copper and Zinc Toxicity in Innate Immune Defense against Bacterial Pathogens. *J Biol Chem* **290**, 18954-18961 (2015).
43. Besold, A.N., Culbertson, E.M. & Culotta, V.C. The Yin and Yang of copper during infection. *J Biol Inorg Chem* **21**, 137-144 (2016).
44. Kapetanovic, R. *et al.* Salmonella employs multiple mechanisms to subvert the TLR-inducible zinc-mediated antimicrobial response of human macrophages. *FASEB J* **30**, 1901-1912 (2016).
45. Hassan, K.A. *et al.* Zinc stress induces copper depletion in *Acinetobacter baumannii. BMC Microbiol* **17**, 59 (2017).
46. Giachino, A. & Waldron, K.J. Copper tolerance in bacteria requires the activation of multiple accessory pathways. *Mol Microbiol* **114**, 377-390 (2020).
47. McDevitt, C.A. *et al.* A molecular mechanism for bacterial susceptibility to zinc. *PLoS Pathog* **7**, e1002357 (2011).
48. Cain, A.K. *et al.* A decade of advances in transposon-insertion sequencing. *Nat Rev Genet* **21**, 526-540 (2020).
49. Langridge, G.C. *et al.* Simultaneous assay of every Salmonella Typhi gene using one million transposon mutants. *Genome Res* **19**, 2308-2316 (2009).
50. Barquist, L. *et al.* The TraDIS toolkit: sequencing and analysis for dense transposon mutant libraries. *Bioinformatics* **32**, 1109-1111 (2016).
51. Alquethamy, S.F. *et al.* The Role of the CopA Copper Efflux System in *Acinetobacter baumannii* Virulence. *Int J Mol Sci* **20** (2019).
52. Alquethamy, S.F. *et al.* The Role of Zinc Efflux during Acinetobacter baumannii Infection. *ACS Infect Dis* **6**, 150-158 (2020).
53. Gallagher, L.A. *et al.* Resources for Genetic and Genomic Analysis of Emerging Pathogen Acinetobacter baumannii. *J Bacteriol* **197**, 2027-2035 (2015).

54. Bhamidimarri, S.P. *et al.* A Multidisciplinary Approach toward Identification of Antibiotic Scaffolds for Acinetobacter baumannii. *Structure* **27**, 268-280 e266 (2019).
55. Kroger, C., Kary, S.C., Schauer, K. & Cameron, A.D. Genetic Regulation of Virulence and Antibiotic Resistance in Acinetobacter baumannii. *Genes (Basel)* **8** (2016).
56. Shannon, P. *et al.* Cytoscape: a software environment for integrated models of biomolecular interaction networks. *Genome Res* **13**, 2498-2504 (2003).
57. Dinh, H., Semenec, L., Kumar, S.S., Short, F.L. & Cain, A.K. Microbiology's next top model: Galleria in the molecular age. *Pathog Dis* **79** (2021).
58. Frei, A. *et al.* Nontoxic Cobalt(III) Schiff Base Complexes with Broad-Spectrum Antifungal Activity. *Chemistry* **27**, 2021-2029 (2021).
59. Caspi, R. *et al.* The MetaCyc database of metabolic pathways and enzymes and the BioCyc collection of pathway/genome databases. *Nucleic Acids Res* **40**, D742-753 (2012).
60. Rumbo-Feal, S. *et al.* Whole transcriptome analysis of *Acinetobacter baumannii* assessed by RNA-sequencing reveals different mRNA expression profiles in biofilm compared to planktonic cells. *PLoS One* **8**, e72968 (2013).
61. Tomaras, A.P., Dorsey, C.W., Edelmann, R.E. & Actis, L.A. Attachment to and biofilm formation on abiotic surfaces by *Acinetobacter baumannii*: involvement of a novel chaperone-usher pili assembly system. *Microbiology (Reading)* **149**, 3473-3484 (2003).
62. Lemke, J.J. *et al.* Direct regulation of *Escherichia coli* ribosomal protein promoters by the transcription factors ppGpp and DksA. *Proc Natl Acad Sci U S A* **108**, 5712-5717 (2011).
63. Pederick, V.G. *et al.* ZnuA and zinc homeostasis in *Pseudomonas aeruginosa*. *Sci Rep* **5**, 13139 (2015).
64. Schneider, D.A., Gaal, T. & Gourse, R.L. NTP-sensing by rRNA promoters in Escherichia coli is direct. *Proc Natl Acad Sci U S A* **99**, 8602-8607 (2002).
65. Gaal, T., Bartlett, M.S., Ross, W., Turnbough, C.L., Jr. & Gourse, R.L. Transcription regulation by initiating NTP concentration: rRNA synthesis in bacteria. *Science* **278**, 2092-2097 (1997).
66. Gourse, R.L., Gaal, T., Bartlett, M.S., Appleman, J.A. & Ross, W. rRNA transcription and growth rate-dependent regulation of ribosome synthesis in *Escherichia coli*. *Annu Rev Microbiol* **50**, 645-677 (1996).
67. Richardson, D.J. Bacterial respiration: a flexible process for a changing environment. *Microbiology (Reading)* **146 (Pt 3)**, 551-571 (2000).
68. Amiott, E.A. & Jaehning, J.A. Mitochondrial transcription is regulated via an ATP "sensing" mechanism that couples RNA abundance to respiration. *Mol Cell* **22**, 329-338 (2006).
69. Farrugia, D.N. *et al.* The complete genome and phenome of a community-acquired Acinetobacter baumannii. *PLoS One* **8**, e58628 (2013).
70. Harwood, C.S. & Parales, R.E. The beta-ketoadipate pathway and the biology of self-identity. *Annu Rev Microbiol* **50**, 553-590 (1996).
71. Fuchs, G., Boll, M. & Heider, J. Microbial degradation of aromatic compounds - from one strategy to four. *Nat Rev Microbiol* **9**, 803-816 (2011).
72. Karp, P.D. *et al.* The BioCyc collection of microbial genomes and metabolic pathways. *Brief Bioinform* **20**, 1085-1093 (2019).
73. Heeb, S. & Haas, D. Regulatory roles of the GacS/GacA two-component system in plant-associated and other gram-negative bacteria. *Mol Plant Microbe Interact* **14**, 1351-1363 (2001).
74. Camacho, M.I. *et al.* Effects of the global regulator CsrA on the BarA/UvrY two-component signaling system. *J Bacteriol* **197**, 983-991 (2015).
75. Chavez, R.G., Alvarez, A.F., Romeo, T. & Georgellis, D. The physiological stimulus for the BarA sensor kinase. *J Bacteriol* **192**, 2009-2012 (2010).

76. de la Peña Mattozzi, d.l.P.M., Kang Y & Keasling, J.D. *Feast: Choking on Acetyl-CoA, the Glyoxylate Shunt, and Acetyl-CoA-Driven Metabolism.* (Springer, Berlin, Heidelberg; 2010).
77. Ahn, S., Jung, J., Jang, I.A., Madsen, E.L. & Park, W. Role of Glyoxylate Shunt in Oxidative Stress Response. *J Biol Chem* **291**, 11928-11938 (2016).
78. McKinney, J.D. *et al.* Persistence of Mycobacterium tuberculosis in macrophages and mice requires the glyoxylate shunt enzyme isocitrate lyase. *Nature* **406**, 735-738 (2000).
79. Meylan, S. *et al.* Carbon Sources Tune Antibiotic Susceptibility in Pseudomonas aeruginosa via Tricarboxylic Acid Cycle Control. *Cell Chem Biol* **24**, 195-206 (2017).
80. Mackie, A.M., Hassan, K.A., Paulsen, I.T. & Tetu, S.G. Biolog Phenotype Microarrays for phenotypic characterization of microbial cells. *Methods Mol Biol* **1096**, 123-130 (2014).
81. Poole, K. Bacterial stress responses as determinants of antimicrobial resistance. *J Antimicrob Chemother* **67**, 2069-2089 (2012).
82. Farr, S.B. & Kogoma, T. Oxidative stress responses in Escherichia coli and Salmonella typhimurium. *Microbiol Rev* **55**, 561-585 (1991).
83. Lacour, S. & Landini, P. SigmaS-dependent gene expression at the onset of stationary phase in Escherichia coli: function of sigmaS-dependent genes and identification of their promoter sequences. *J Bacteriol* **186**, 7186-7195 (2004).
84. Kandror, O., DeLeon, A. & Goldberg, A.L. Trehalose synthesis is induced upon exposure of Escherichia coli to cold and is essential for viability at low temperatures. *Proc Natl Acad Sci U S A* **99**, 9727-9732 (2002).
85. Aberg, A., Fernandez-Vazquez, J., Cabrer-Panes, J.D., Sanchez, A. & Balsalobre, C. Similar and divergent effects of ppGpp and DksA deficiencies on transcription in *Escherichia coli*. *J Bacteriol* **191**, 3226-3236 (2009).
86. Dwyer, D.J. *et al.* Antibiotics induce redox-related physiological alterations as part of their lethality. *Proc Natl Acad Sci U S A* **111**, E2100-2109 (2014).
87. Lobritz, M.A. *et al.* Antibiotic efficacy is linked to bacterial cellular respiration. *Proc Natl Acad Sci U S A* **112**, 8173-8180 (2015).
88. Zhang, B. *et al.* NMR analysis of a stress response metabolic signaling network. *J Proteome Res* **10**, 3743-3754 (2011).
89. Nguyen, D. *et al.* Active starvation responses mediate antibiotic tolerance in biofilms and nutrient-limited bacteria. *Science* **334**, 982-986 (2011).
90. Maharjan, R. *et al.* The form of a trade-off determines the response to competition. *Ecol Lett* **16**, 1267-1276 (2013).
91. Flynn, J.M., Neher, S.B., Kim, Y.I., Sauer, R.T. & Baker, T.A. Proteomic discovery of cellular substrates of the ClpXP protease reveals five classes of ClpX-recognition signals. *Mol Cell* **11**, 671-683 (2003).
92. Macomber, L. & Imlay, J.A. The iron-sulfur clusters of dehydratases are primary intracellular targets of copper toxicity. *Proc Natl Acad Sci U S A* **106**, 8344-8349 (2009).
93. Tucker, A.T. *et al.* Defining gene-phenotype relationships in *Acinetobacter baumannii* through one-step chromosomal gene inactivation. *mBio* **5**, e01313-01314 (2014).
94. Adams, F.G., Stroeher, U.H., Hassan, K.A., Marri, S. & Brown, M.H. Resistance to pentamidine is mediated by AdeAB, regulated by AdeRS, and influenced by growth conditions in *Acinetobacter baumannii* ATCC 17978. *PLoS One* **13**, e0197412 (2018).
95. Seemann, T. (https://github.com/tseemann/snippy).
96. Herrero, M., de Lorenzo, V. & Timmis, K.N. Transposon vectors containing non-antibiotic resistance selection markers for cloning and stable chromosomal insertion of foreign genes in gram-negative bacteria. *J Bacteriol* **172**, 6557-6567 (1990).
97. Fabian, B.K. *et al.* Elucidating Essential Genes in Plant-Associated *Pseudomonas protegens* Pf-5 Using Transposon Insertion Sequencing. *J Bacteriol* **203** (2021).

98. Keseler, I.M. *et al.* The EcoCyc database: reflecting new knowledge about *Escherichia coli* K-12. *Nucleic Acids Res* **45**, D543-D550 (2017).
99. Loh, J.M., Adenwalla, N., Wiles, S. & Proft, T. Galleria mellonella larvae as an infection model for group A streptococcus. *Virulence* **4**, 419-428 (2013).
100. O'Toole, G.A. Microtiter dish biofilm formation assay. *J Vis Exp* (2011).
101. Kon, H., Schwartz, D., Temkin, E., Carmeli, Y. & Lellouche, J. Rapid identification of capsulated *Acinetobacter baumannii* using a density-dependent gradient test. *BMC Microbiol* **20**, 285 (2020).

Figures

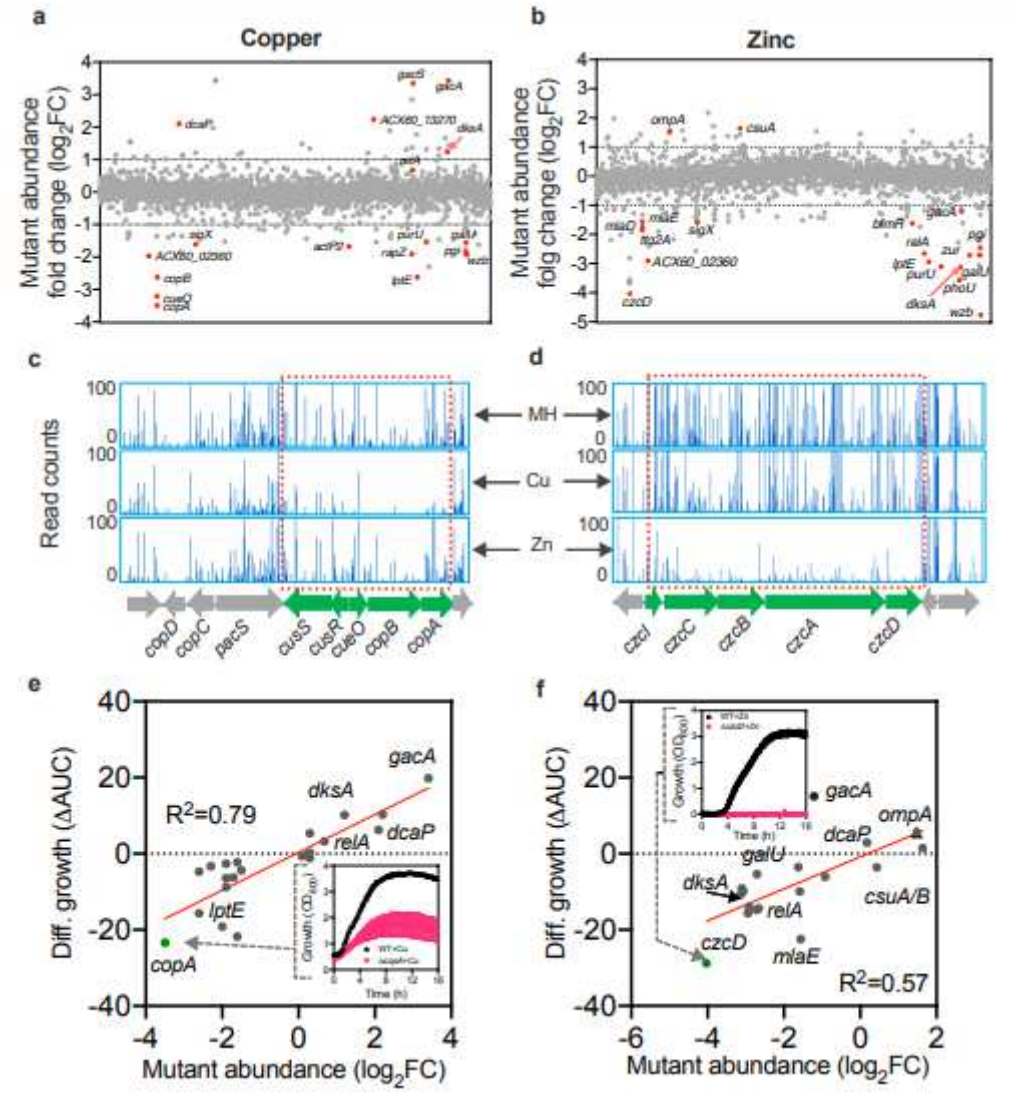

Figure 1

Identification and validation of A. baumannii genes that alter fitness under copper and zinc stresses using the TraDIS approach.

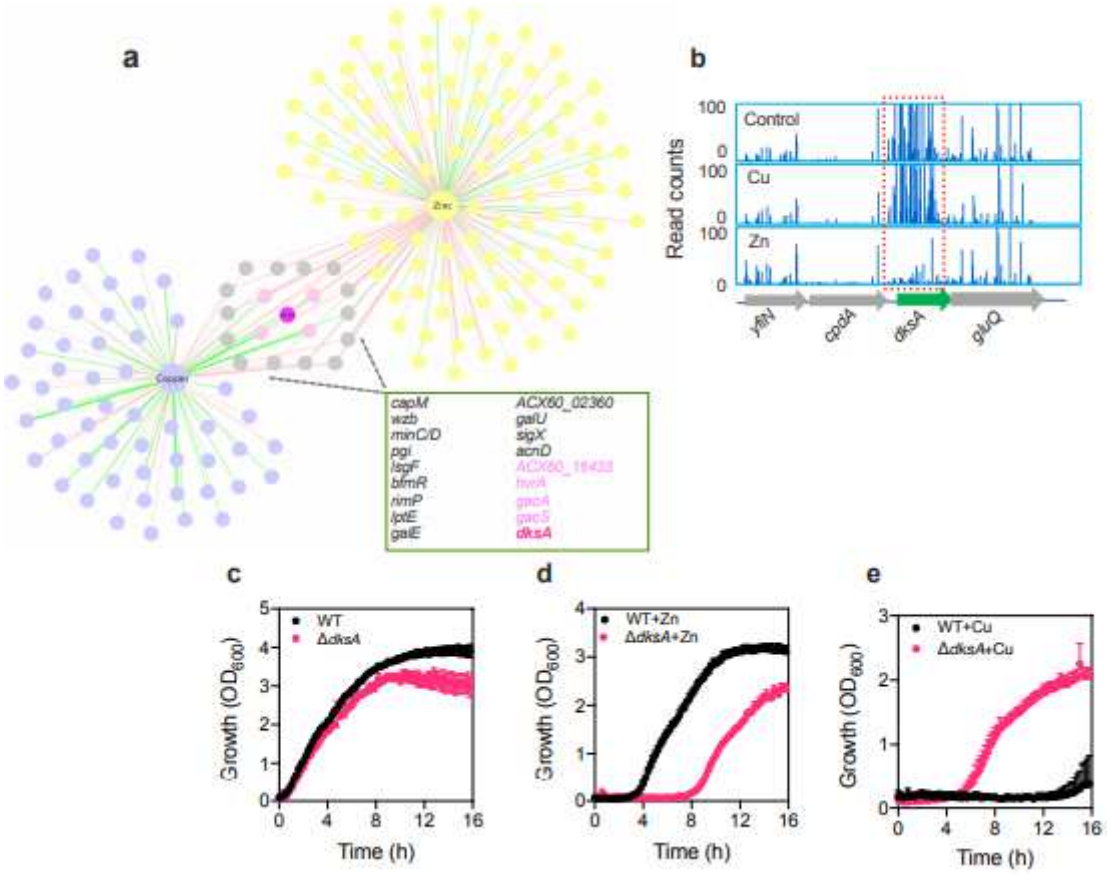

Figure 2

DksA has an opposite role in zinc and copper stress protection.

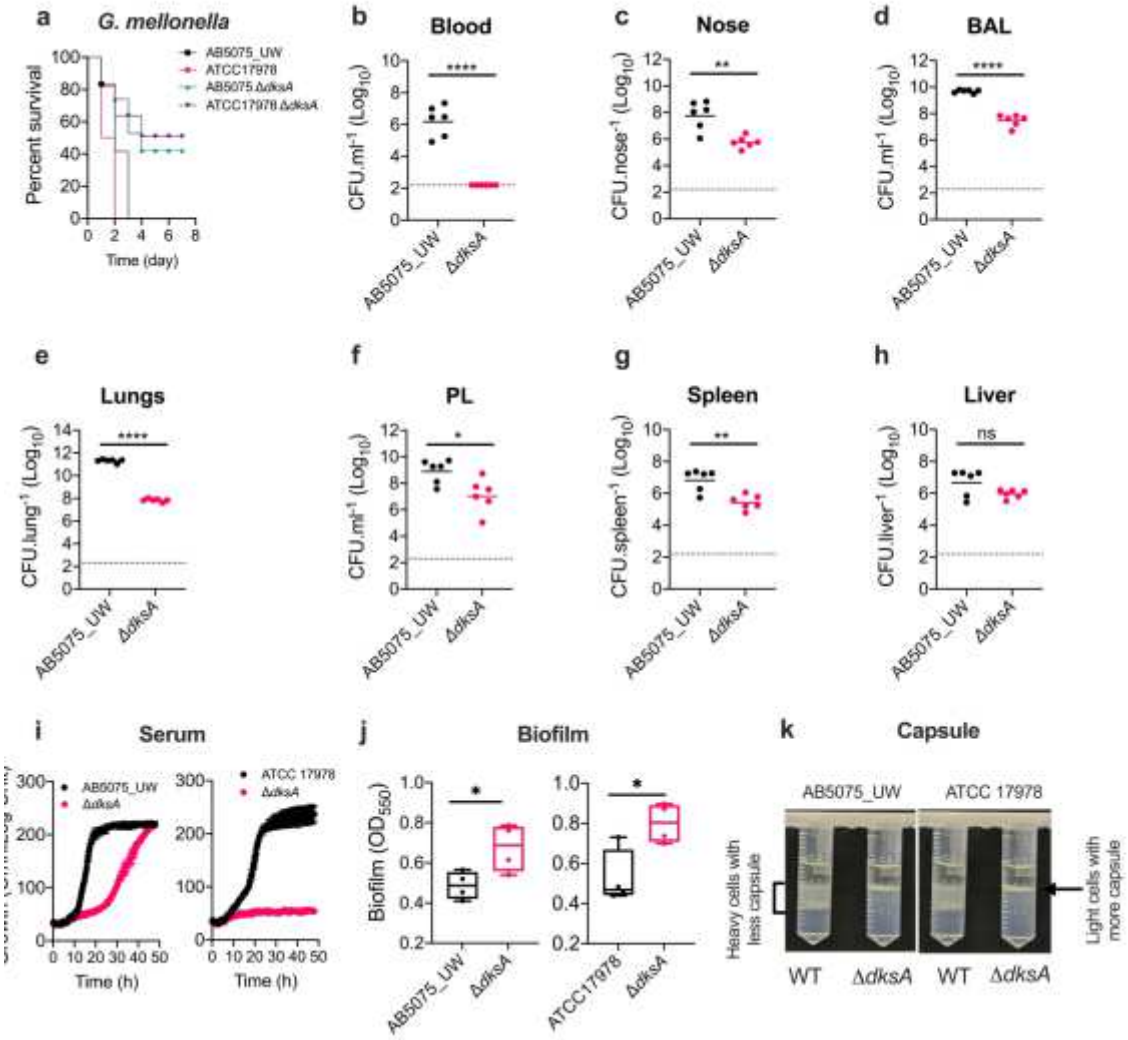

Figure 3

DksA-dependent virulence and niche specific colonization of A. baumannii and associated phenotype.

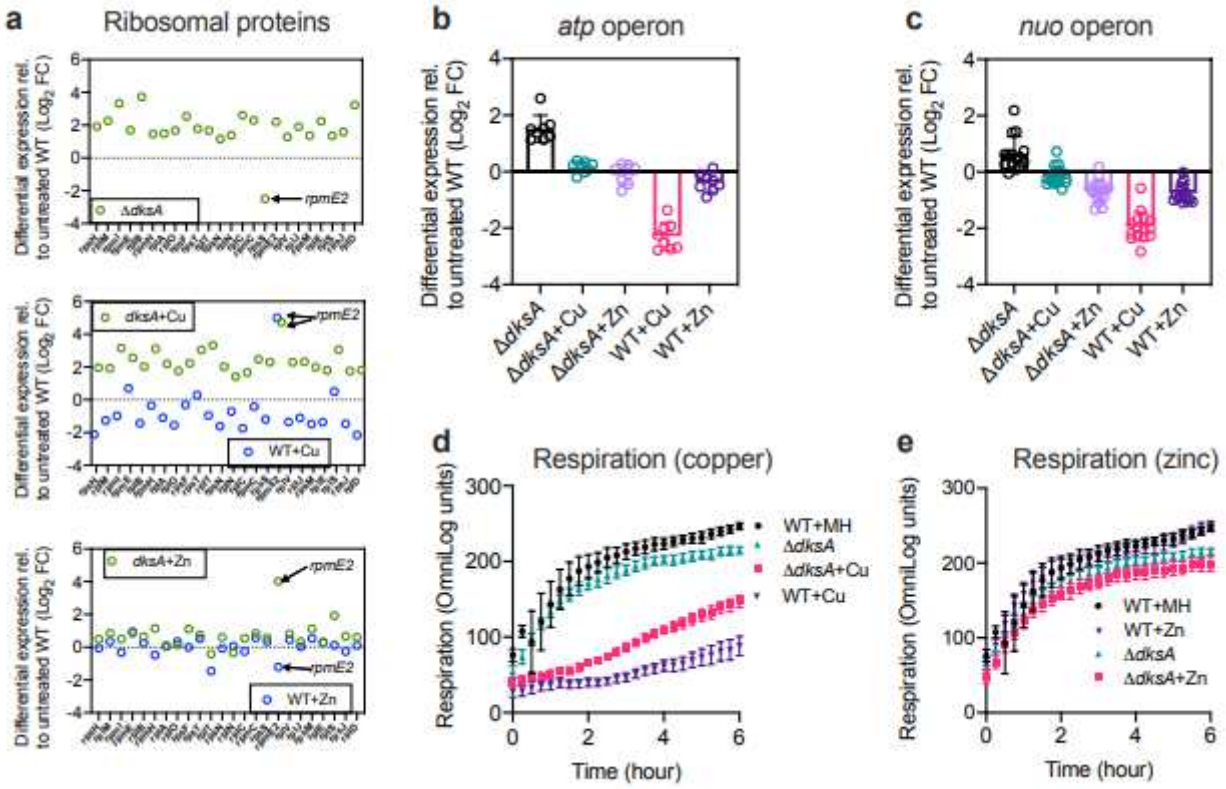

Figure 4

Copper stress attenuates expression of ribosomal protein and respiratory genes in A. baumannii in a DksA dependent manner.

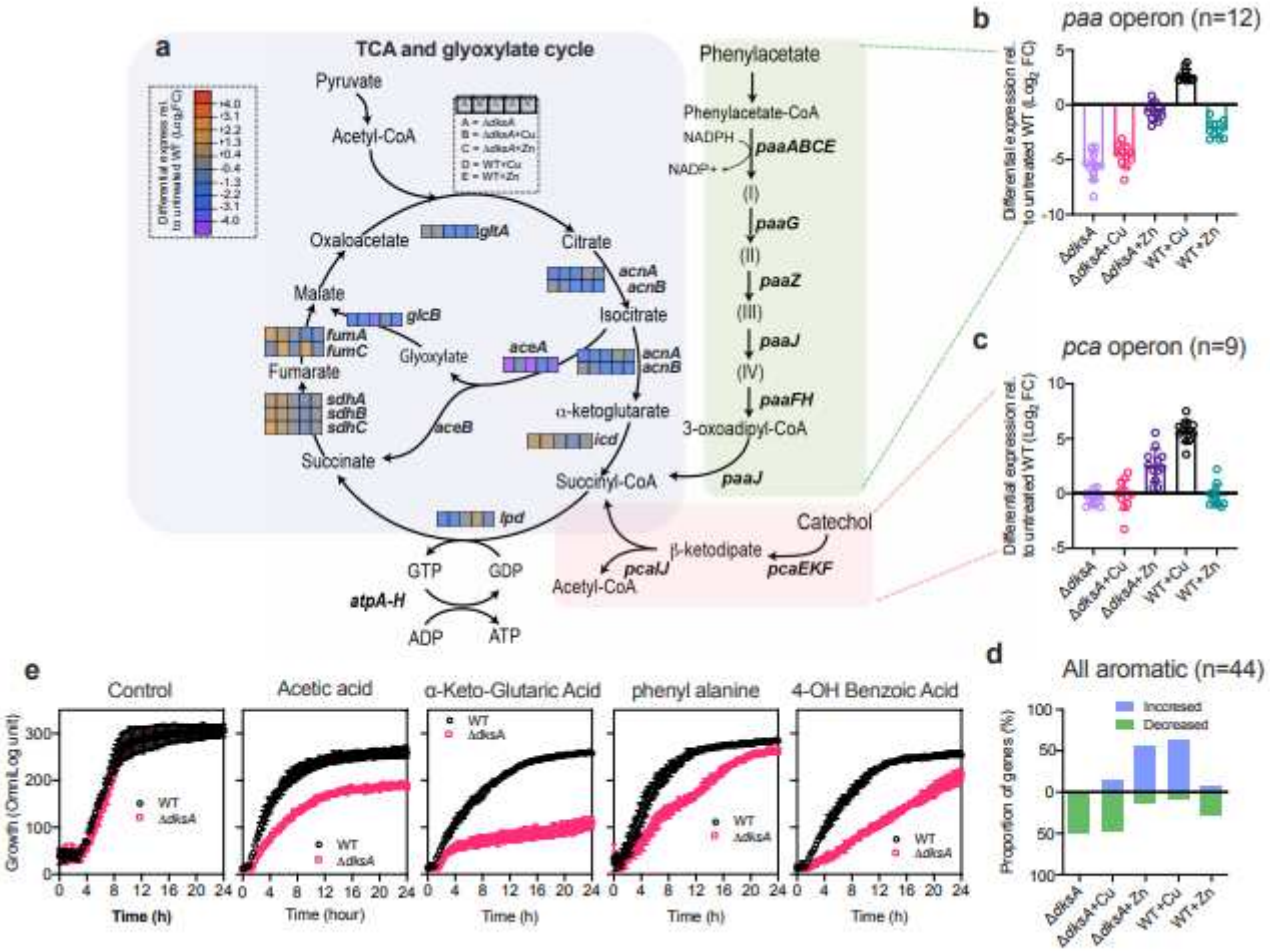

Figure 5

DksA regulates phenylacetate, β-ketoadipate and TCA-glyoxylate pathways in A. baumannii.

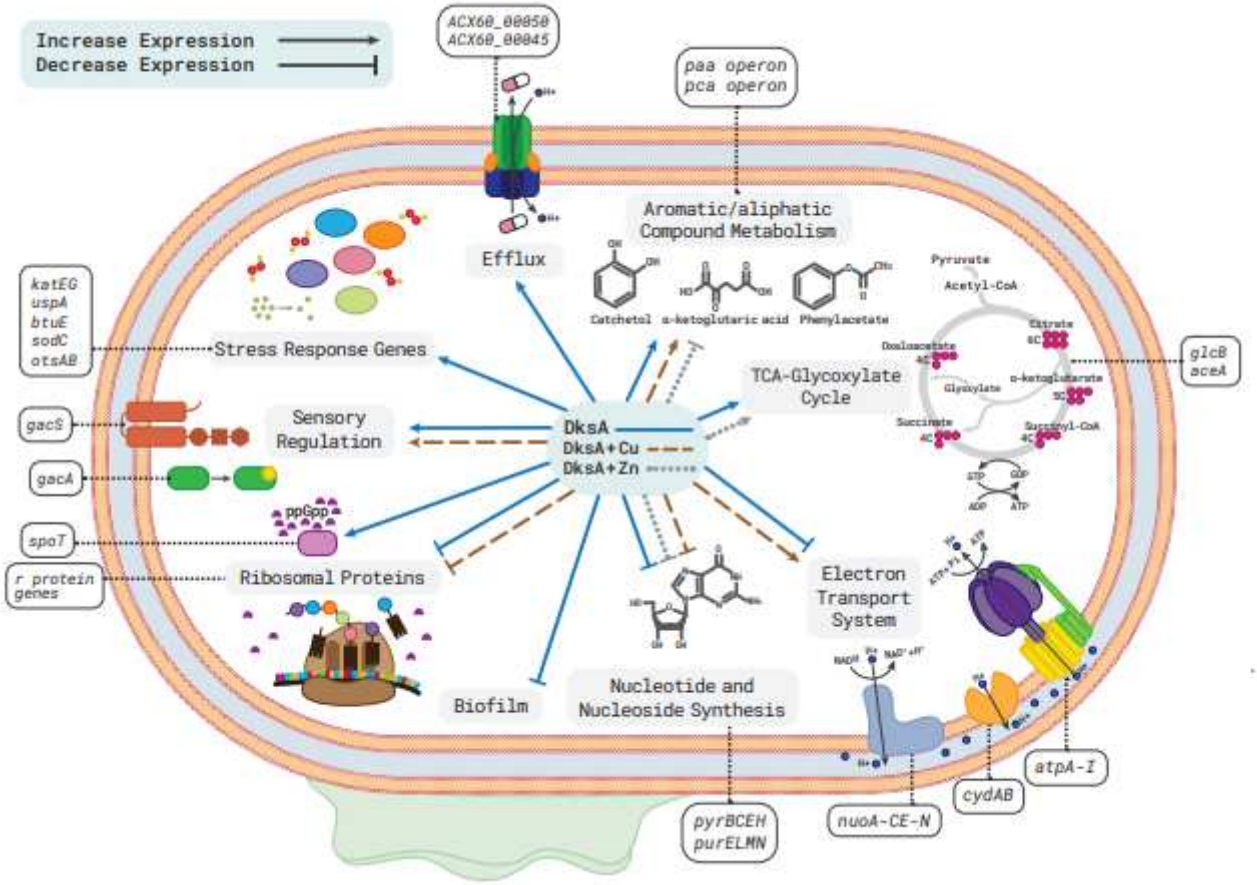

Figure 6

An overview of DksA-dependent stress regulation in A. baumannii.

Supplementary Files

This is a list of supplementary files associated with this preprint. Click to download.

- Supplementarymaterial.pdf
- Supplemtarytables1and2.xlsx